

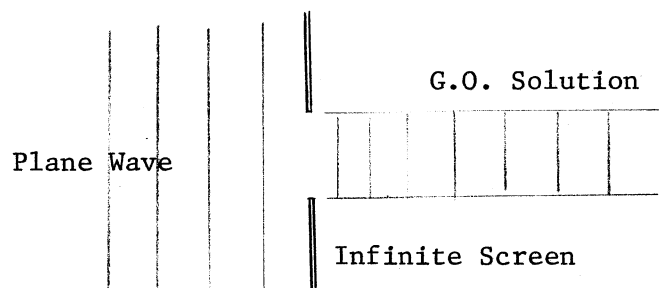
GEOMETRIC THEORY OF DIFFRACTION (GTD)

This is a method of extending geometric optics solutions to field problems by including diffractions from edges and curved surfaces. The field at a point is the vector phasor sum of the various components from all possible direct, reflected, and diffracted fields from sources of radiation. These fields propagate from the sources as ray optics fields. Once expressions are found for the various types of diffractions, the problem reduces to tracing rays and accounting for all possible sources at a given field point. Because the contribution of each part of the total field can be separated, a great deal of insight into the importance of each structure can be gained. Sources of trouble can be identified and work concentrated on those areas. In those cases where the field can be found by eigenvalue problems involving partial differential equations, the contribution of any one part is lost in the solution. Contributions cannot be separated.

GTD is inherently a high frequency technique which has been extended by diffraction coefficients so that many problems on the order of one wavelength can be accurately solved and valid engineering solutions found for structures as small as $\lambda/4$. Eigenvalue solutions are quite limited because as the size increases more and more modes are required to accurately describe the field. Usually to solve the partial differential equations, it is necessary for the structure to fit some standard coordinate system. Of course, we can use any set of eigenfunctions to expand the fields and find a solution using moment methods. GTD cannot replace these important methods but it is bounded by zero wavelength on one end (GO) and extends into the region covered by moment methods. In fact, moment methods have been combined with GTD to improve the accuracy in the transition region.

SLIT IN A SCREEN

Suppose there is an infinite screen with a slit in it and a plane wave incident from the left as shown below. Consider the possible solutions.



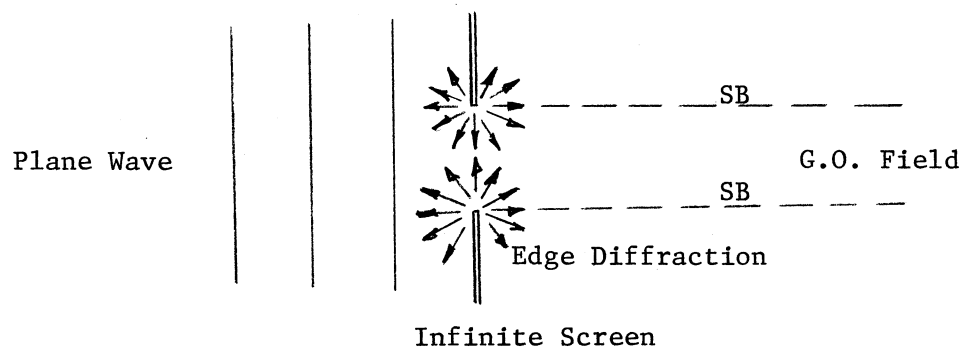
A geometric optics solution gives us a column field on the right side of the screen as shown above. Note that all the solutions can be described in two dimensional space. When the width of the slot is large in terms of wavelengths, there are distinct shadows and G.O. is valid or at least approximately. As the slot width is reduced we must consider aperture diffraction.

Historically the first method is the Huygens source approximation. Each point in the aperture can be considered a source of waves. This is a two dimensional problem so the waves are cylindrical. The solution for the far field is given by the Fourier transform of the fields in the aperture. This

is discussed thoroughly on page 530. Because the screen is still present after the induction theorem as been applied to find the aperture fields, the solution is not valid near the screen. Nothing has been done to satisfy the boundary conditions imposed by the screen. We get the $\sin X/X$ pattern in k space for the uniform aperture field.

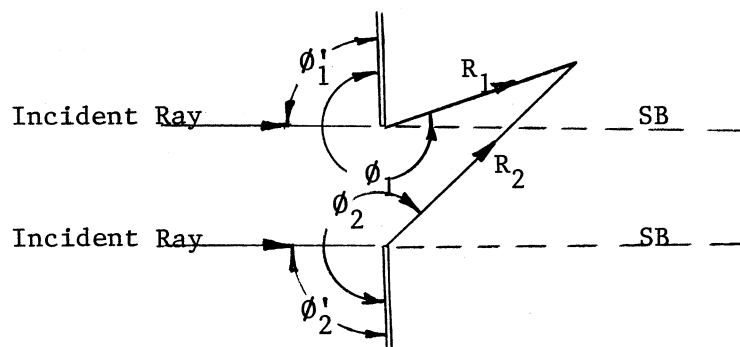
In the next method equivalent currents are found in the aperture using the equivalence theorem and replace the aperture fields. The aperture can be replaced by a metal screen and the method of images can be used to find the exact fields on the right side of the aperture. This method requires an exact knowledge of the fields in the aperture. When geometric optics are used to find the fields, the solution is called the physical optics approximation. This method was used to find the radiation from a slot on page 176. Vector potentials are used with the equivalent currents to find the radiation. In as much as the fields are known in the aperture, the method can find near and far fields.

GTD combines the geometric optics solution with diffractions from the two edges. These diffractions are dependent on the direction of the diffraction.



The lines labeled SB are the shadow boundaries where the G.O. field vanishes. The diffractions will be discontinuous across the boundary to compensate for the discontinuity in the G.O. field because the total field will be continuous across the boundary. The GTD solution will not only predict the fields on the right side of the screen, but also the left. The diffractions have identifiable sources: the edges of the slot.

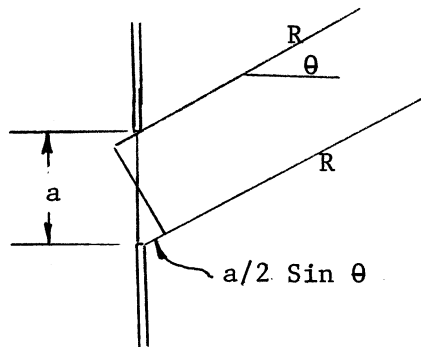
Consider a point at which the field is to be found and the ray tracing to it.



In the diagram above there is no contribution by the G.O. field but only the diffractions. The amplitude of the diffractions depends on the angles ϕ' and ϕ and the distances R_i . The diffractions are no longer plane waves as the

incident wave, but cylindrical waves whose radius of curvature is at the point of diffraction. It is the caustic of the wave. The phase is determined by the diffraction coefficient and the distance R_1 because it is assumed that the diffraction rays are ray optic (free space) waves. Since R_1 and R_2 are finite, we can find the near field of the diffraction and the waves which are diffracted on the incident side of the screen. At this point we will not concern ourselves with the details of the diffraction coefficients, but only the idea. They are found from a solvable canonical problem and extended to other cases.

As we extend the distances R_1 and R_2 further and further, we must evolve the solution into a far field formulation. The amplitude becomes proportional to $1/R$ but the phase difference remains like any other far field approximation. We have a two element array with the edges as the elements whose patterns are not identical.



The problem can be solved, in theory, without resorting to a far field approximation, but since the diffraction coefficients are usually found by computer routines, to maintain accuracy it is necessary to use it. When R becomes large, it would be necessary to find the sine and cosine of large numbers.

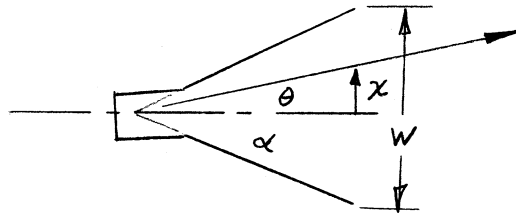
$$e^{-j k R} = \cos(kR) - j \sin(kR)$$

The computer with a finite word length soon loses all significant digits and the results are based on the evaluation of functions with one or two significant digits. Although GTD can find both the far field and the near field, we are forced in many cases to formulate the problems in separate ways.

One of the possible diffractions is from one edge to the other. Now instead of a plane wave incident on the edge, we have a cylindrical wave. This wave will be diffracted by the edge and give another contribution to the total field. But this diffraction is quite a bit smaller than the first diffraction. This process can be repeated again and again to get higher order diffractions, but the contributions diminish rapidly. It is also possible to take all multiple diffractions together and find a self consistent set of waves between the two edges which account for all the multiple diffractions and gives simple amplitudes for the incident waves. Unless the edges are close together, double diffraction will give the best results. We will find that it is not necessary to consider all possible low order diffractions for all parts of the pattern. GTD will show by discontinuities in the pattern that additional terms are necessary. Sometimes small discontinuities are unimportant and not worth the extra effort to remove.

GEOMETRIC OPTICS OF ANTENNAS

Geometric optics is a high frequency approximation which has distinct shadows. Consider a horn antenna as shown below. The horn has a flare



angle of 2α . The G.O. solution is radiation which has a caustic at the projected intersection of the two slant sides and spreads within the 2α region and does not escape. The G.O. field is a pyramid whose tip is determined by the sides of the horn. In the case of the E plane, it is of constant amplitude and a cosine distribution in the H plane since the field vanishes on the walls. The phase is determined by the distance to the vertex. The cosine distribution is in terms of the variable X in the figure above and we should express it in terms of the angle θ . The aperture field distribution is

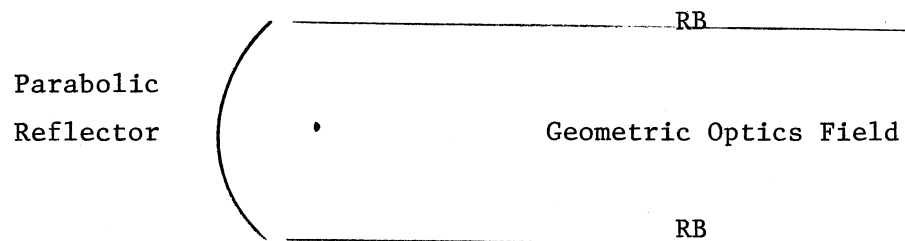
$$K \cos(\pi X/W)$$

If the axial length is L , then $W = 2 L \tan \alpha$. For a given θ , the aperture distance, $X = L \tan \theta$. Using these the G.O. field in the aperture becomes

$$K \cos\left(\frac{\pi \tan \theta}{2 \tan \alpha}\right)$$

The far field will also require a ray phase term: e^{-jkR_0} and an amplitude term: $1/R_0$ for spherical waves or $1/\sqrt{R_0}$ for cylindrical waves.

The parabolic reflector has a simple G.O. field. The spherical waves from the feed at the focus are converted into plane waves in the aperture. The solution is a column of plane waves from the projection of the dish outer curve.



The caustic for this wave is at infinity which means that neither G.O. or GTD can predict the far field at boresight since both fail at caustics. The GTD problem can be solved by finding equivalent rim currents to account for the diffractions. The vector potential is used to find the fields. But most times the field at boresight is not needed or can be found easily using aperture techniques.

The geometric optics of shaped reflectors can be found by the intermediate results of the synthesis. In one case the wave is spread without a caustic and in the other the caustic is near the antenna. The far field pattern can

be found everywhere. The amplitude of the beam in various directions was a given function and is still valid. The point of reflection was found by using normalized energy integrals to relate the source angle to the reflection point. Knowing the reflection point and the field point we can find the path length through reflection. The total phase is given by the factor

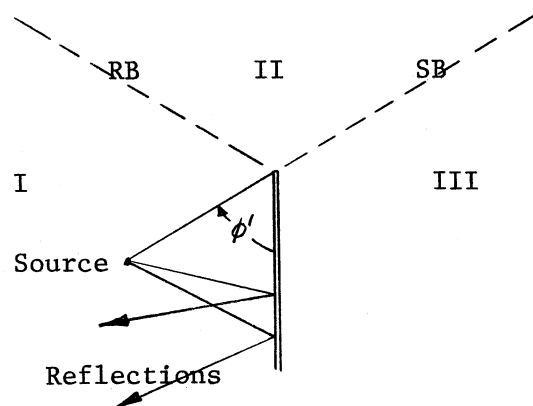
$$e^{-j k (\rho(\phi) + R(\phi))}$$

where ρ is the distance from the feed to the antenna and $R(\phi)$ is the distance from the reflector to the far field point.

After reflection from a curved surface, the radii of curvature of the wave changes. Expressions are needed to relate the radii of curvature of the incident wave and the radii of curvature of the reflector to the radii of curvature of the output wave. But in the case of the synthesized reflector, these were already given in the procedure to design the surface. In the general reflector it is necessary to search for the reflection point or points and to determine the change in the radii of curvature of the reflected wave to find the amplitude of the wave at the field point. Through these reflections we still assume that the wave is a free space (ray optic) wave and the phase is determined by the distance.

SHADOWS

Geometric optics predicts perfect shadows. But there cannot be a discontinuity of the fields in space without supporting currents and charges on a surface. The edge of the shadow cannot support currents or charges, therefore the fields must be continuous across the shadow. Consider a semi-infinite ground plane and a line source nearby.

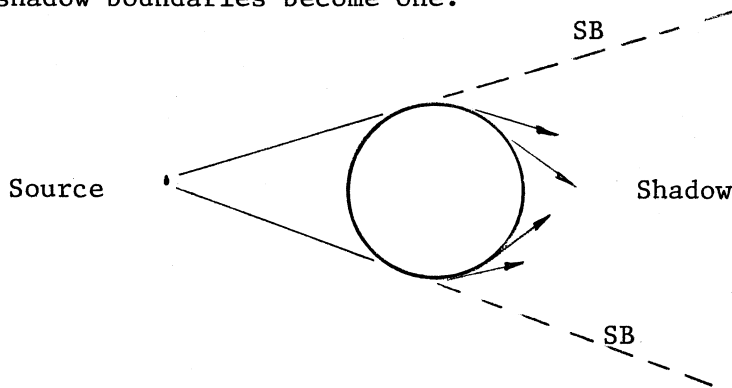


The ground plane will reflect waves as long as the angle ϕ' is large enough that the ray hits the plate. Because of the edge there is a maximum reflection angle, labeled RB (reflection boundary). This is a second discontinuity in the G.O. field and it cannot support currents or charges anymore than the shadow boundary. The fields must be continuous across this boundary as well. The continuity of the fields across these two boundaries is provided by the diffraction coefficient of the edge.

The reflection boundary, RB, and the shadow boundary, SB, divide space into 3 regions. In region I where the source is located and before the RB, there are 3 contributions to the fields; direct, reflected, and diffracted rays.

Region II between the RB and the SB has contributions from direct radiation and diffracted waves. Beyond the SB into region III both the direct and reflected rays are blocked and there is only diffracted waves.

A second type of shadows comes from a smooth object such as the cylinder. Here there is no sharp edge to generate edge diffraction and the reflection and shadow boundaries become one.



There are only two regions of space. Just as before the field must be continuous across the shadow boundary. The GTD solution is given in terms of creeping waves which follow the curved surface and shed energy tangentially.

TYPES OF GTD PROBLEMS

GTD will handle any antenna problem where the dimensions of the pieces are on the order of one wavelength or larger. The types of problems are limited only by the availability of suitable diffraction coefficients. Subject to these restrictions, it can be used for any field problem.

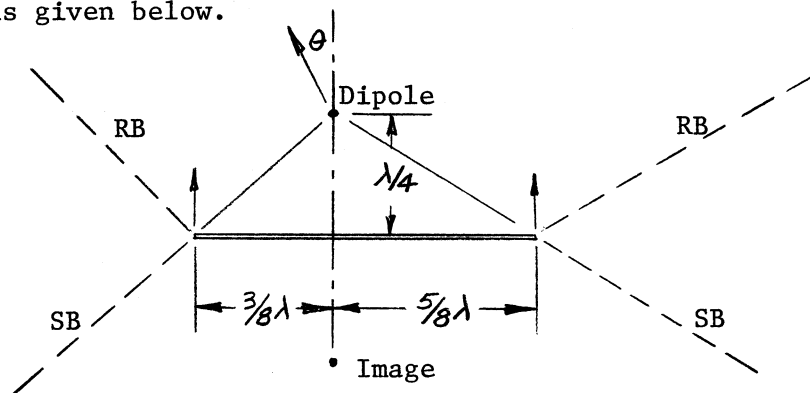
GTD is used to find the pattern of antennas such as horns or corner reflectors where the antenna can be described by flat plates. Usually the problem can be solved by an equivalent 2 dimensional problem which is valid in one plane. Not only is the front lobe of the antenna found, but the backlobe as well. Another common antenna which is solved by GTD is the parabolic reflector. The diffractions off the edges are used to find the pattern off boresight through to the backlobe (except for the exact backlobe) behind the reflector. Small antennas are modelled by simple elements or possibly an array of simple elements whose magnitudes and phases are found from moment methods. The aperture impedance and coupling between antennas can be found in some cases by using GTD.

The other common use of GTD is modelling. The effects of nearby structures can be found by considering the reflections, blockage, and diffractions from edges and curved objects. Aircraft, ships, and missiles are modelled with antennas mounted in various locations. In these cases the antennas are modelled by simple radiators since we are mostly interested in the effects of the structure. But if we are interested in the coupling between, then we must model the antennas more carefully. GTD can also be used to find the scattering off models which means it is suitable for radar cross section calculations.

A common problem is locating a new antenna on an aircraft or ship. All the

prime locations have been taken and there only remains a few locations. GTD can be used to model the vehicle and various locations tried to determine the best location. The antenna can be quickly moved to the possible locations and a determination made without waiting for a model to be built and tested. It is nice to verify the calculated result with measurements, but as confidence in the GTD model is gained, it will be unnecessary to build a model. Too often a decision must be quickly before a model can be made.

Many of the methods of GTD can be given in a simple example. Suppose we have a dipole over a one wavelength ground. We will consider only the H plane. The geometry is given below.



The problem can be handled in 2 dimensions. The electric field is out of the paper and is radiated uniformly around the dipole. Consider the direct radiation. It will be blocked by the ground plane and radiates to the SB, shadow boundary as shown above. The pattern of the direct radiation is given on page 707.

The electric field will be zero at the ground plane from boundary conditions for the tangential electric field. This can be satisfied by an image dipole a quarterwave below and 180° out of phase. The image is the reflected wave and radiates between the reflection boundaries, RB, shown above. The pattern of the reflected signal is drawn on page 707. It is the same amplitude as the direct radiation. We can combine these as a two element array and obtain the pattern shown on page 708. The pattern has discontinuities because we have not taken into account enough sources to get an acceptable pattern. On page 709 is the pattern of a dipole over a 5 wavelength ground plane along with the pattern obtained from considering only the direct and reflected rays. The simple analysis gives accurate patterns out to 80° . It also points out one of the characteristics of GTD. If not enough sources of radiation are considered, then there will be obvious discontinuities in the pattern. For any applications we may not be interested in the areas near the discontinuity and it may not be worth the effort to remove them.

The diffractions from the edges are shown on page 710 referenced to the level of the total pattern. When we combine the edge diffractions with the direct and reflected rays, we have a four element array. Each element has a different

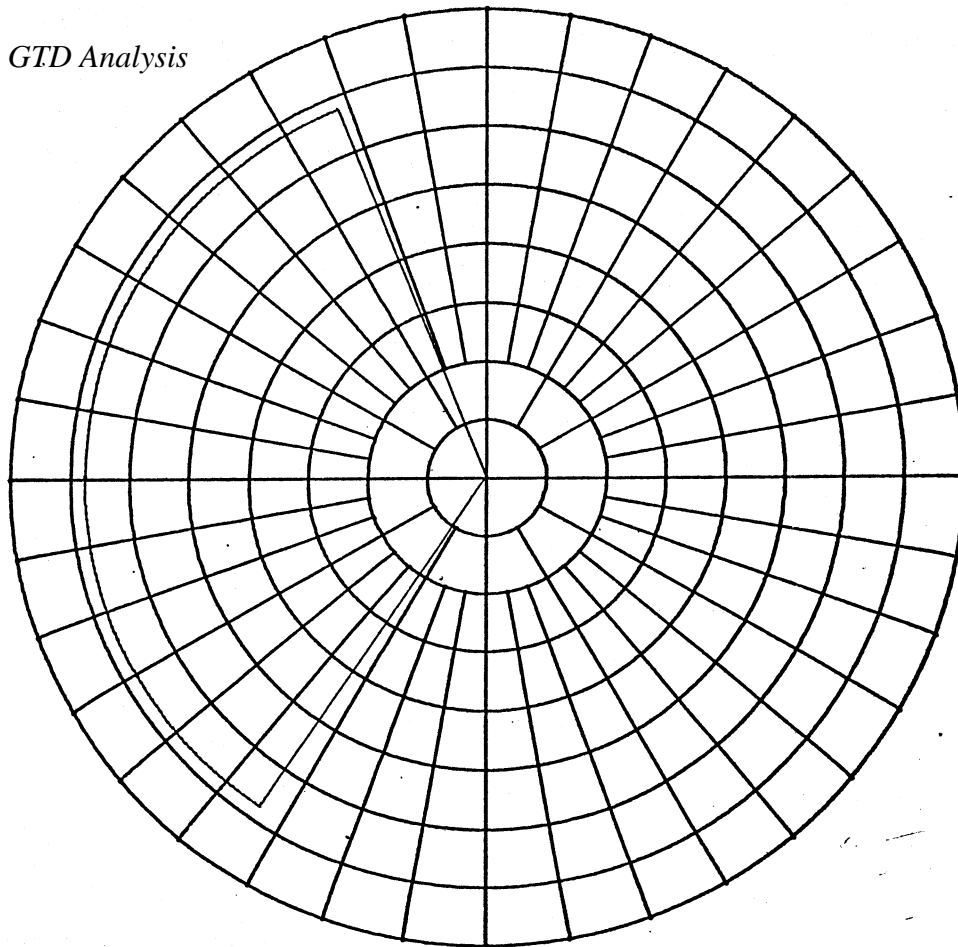
• Dipole

Edge Diffraction •

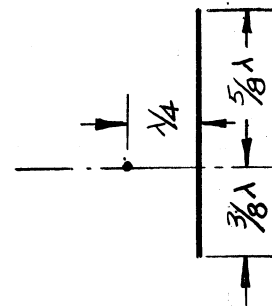
• Edge Diffraction

• Image

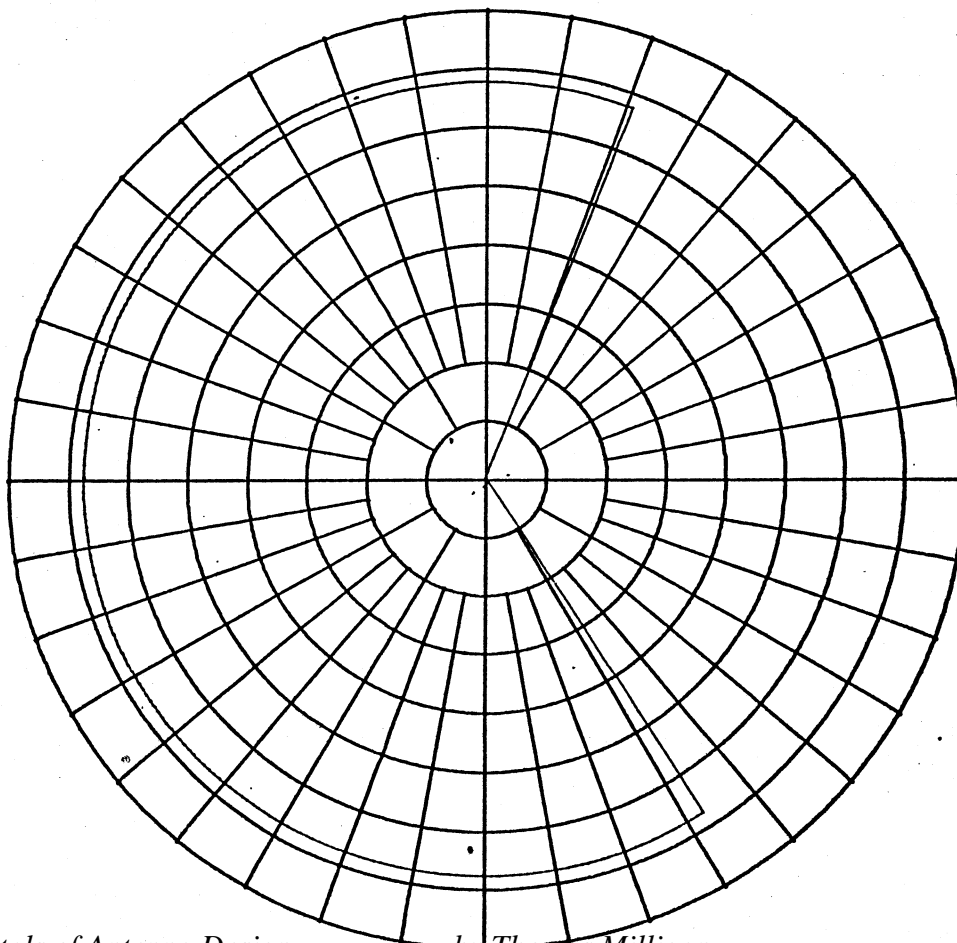
Reflected Field



Dipole over a Ground Plane



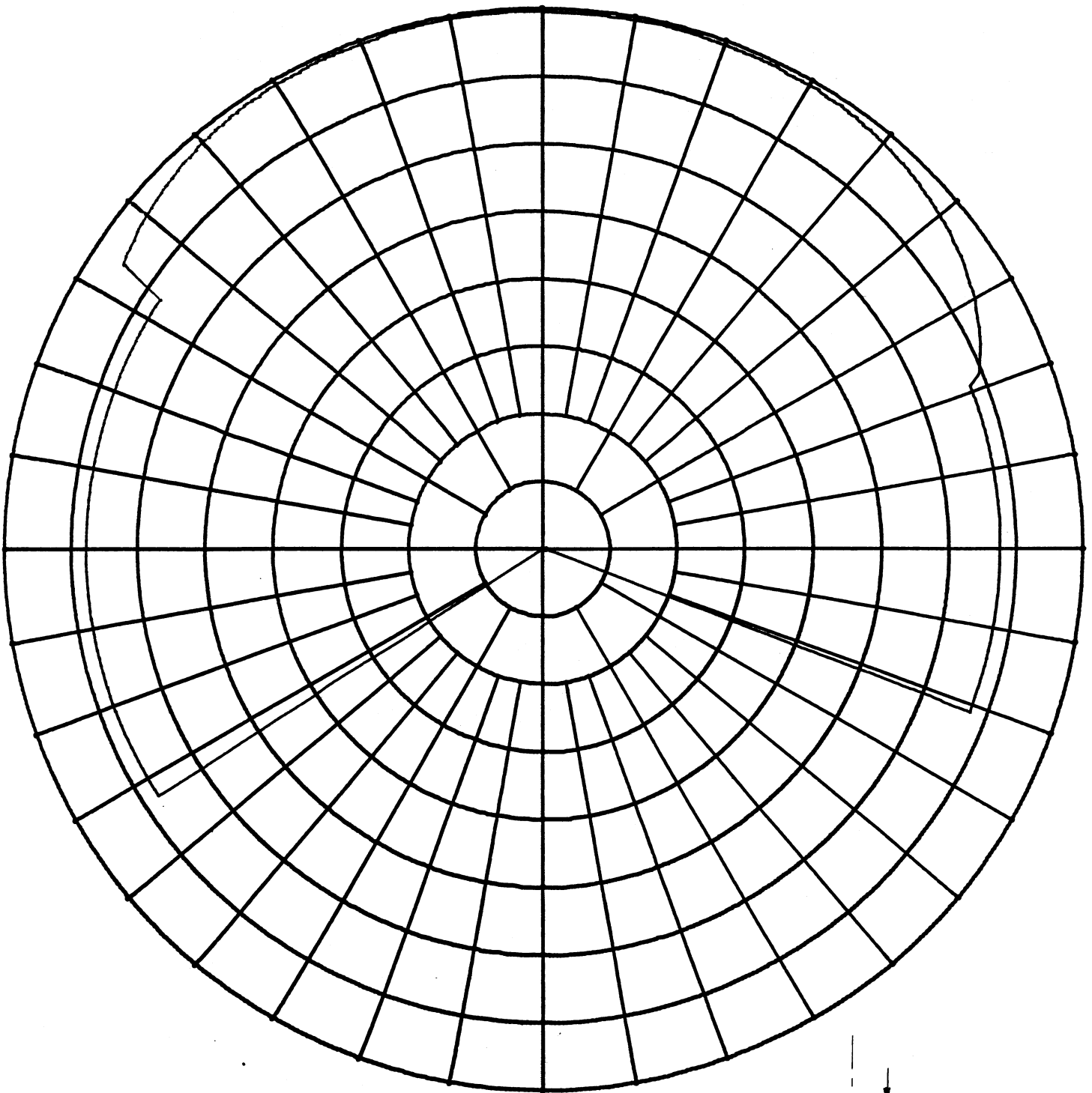
Direct Field



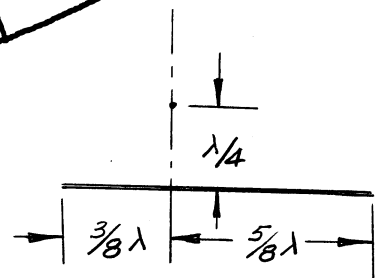
H Plane Pattern of a

H Plane of Dipole Over Ground Plane

Direct + Reflected

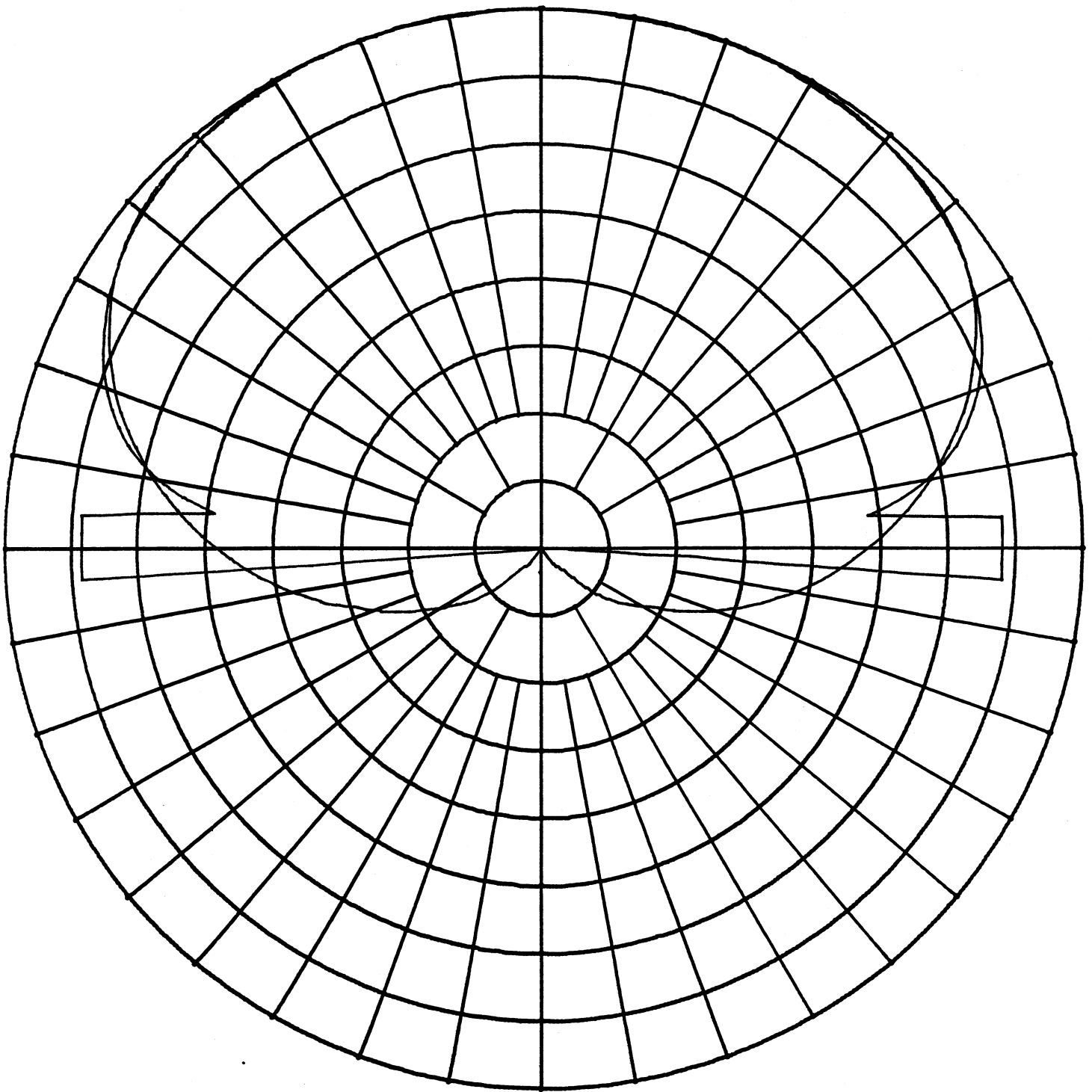


708

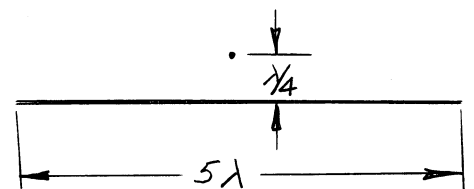


H Plane of a Dipole over a 5 Ground Plane

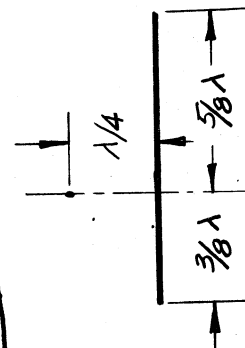
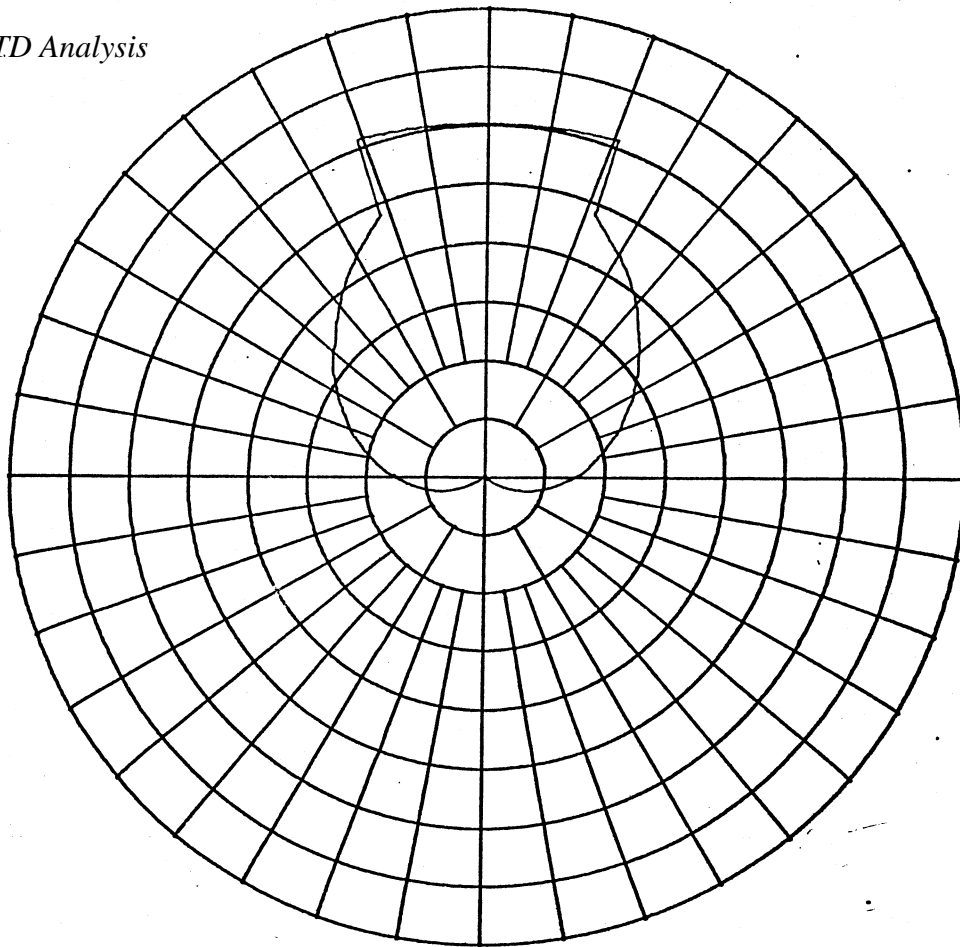
Comparison of Direct + Reflected to Total



709

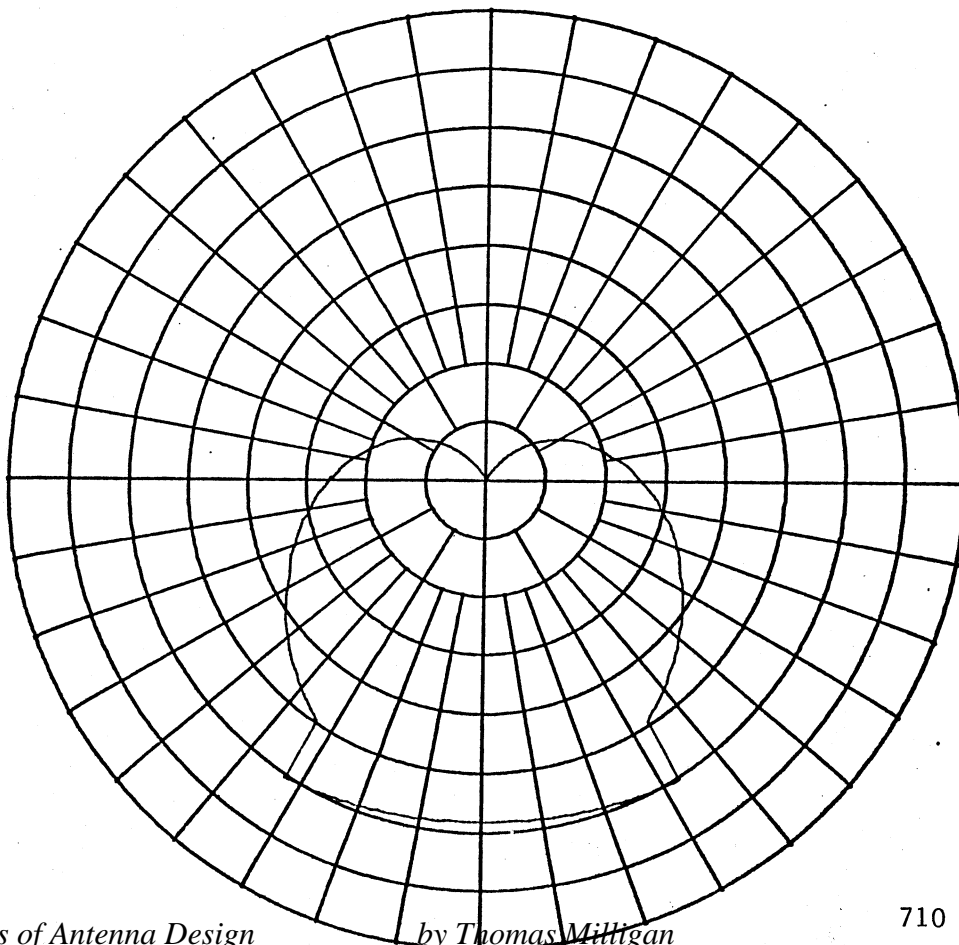


Edge Diffraction



H Plane Pattern of Dipole over a Ground Plane

Edge Diffraction



pattern as been shown. The edge diffraction has discontinuities which compensate for the discontinuities in the combination of reflected and direct rays. The total combination is plotted on page 712. The asymmetry of the ground plane can be seen in the pattern. At $\theta = \pm 90^\circ$ the difference is 2 dB. The phase of the edge diffraction is determined by two factors: first, the wave travels from the source to the edge giving an incident wave with phase: $-kR$. Second, the diffraction coefficient has a phase pattern which has been suppressed in the amplitude only patterns.

Consider the discontinuity at 56° on page 708 in the direct and reflected array. The diffraction from the left edge subtracts from this pattern for $\theta < 56^\circ$; changes sign at $\theta = 57^\circ$; and starts adding to the total pattern. At the second transition, 124° , it again changes sign to smooth out the discontinuity there and form the backlobe. The same thing happens on the other side.

To complete the study of the H plane pattern of a dipole over a ground plane a number of patterns have been drawn on page 713. In all these cases the dipole is a quarter wave over the ground plane.

GEOMETRIC OPTICS

We have considered the general idea of GTD. The major portion of the work solving a problem is geometric optics. We will spend a great deal of time on the forms of various diffraction coefficients, but the bulk of the time solving any problem is spent on geometry and geometric optics. Every diffraction becomes a new source of radiation which must be ray traced through the geometry to the field point. Keeping track of polarization also consumes effort because coordinates must be constantly rotated to match reflection and diffraction boundaries.

We discussed the general astigmatic ray on page 581. It has different radii of curvature in the two principle planes. Remember that the principle planes of a surface at a point are orthogonal and contain the largest and smallest radii of curvature. The electric field has the following variation:

$$E(d) = E_0 e^{-jk d} \sqrt{\frac{\rho_1 \rho_2}{(\rho_1 + d)(\rho_2 + d)}}$$

where E_0 is the phasor of the electric field at $d = 0$, and ρ_1 and ρ_2 are the principle radii of curvature of the ray. The phase factor says that the wave travels like a free space wave.

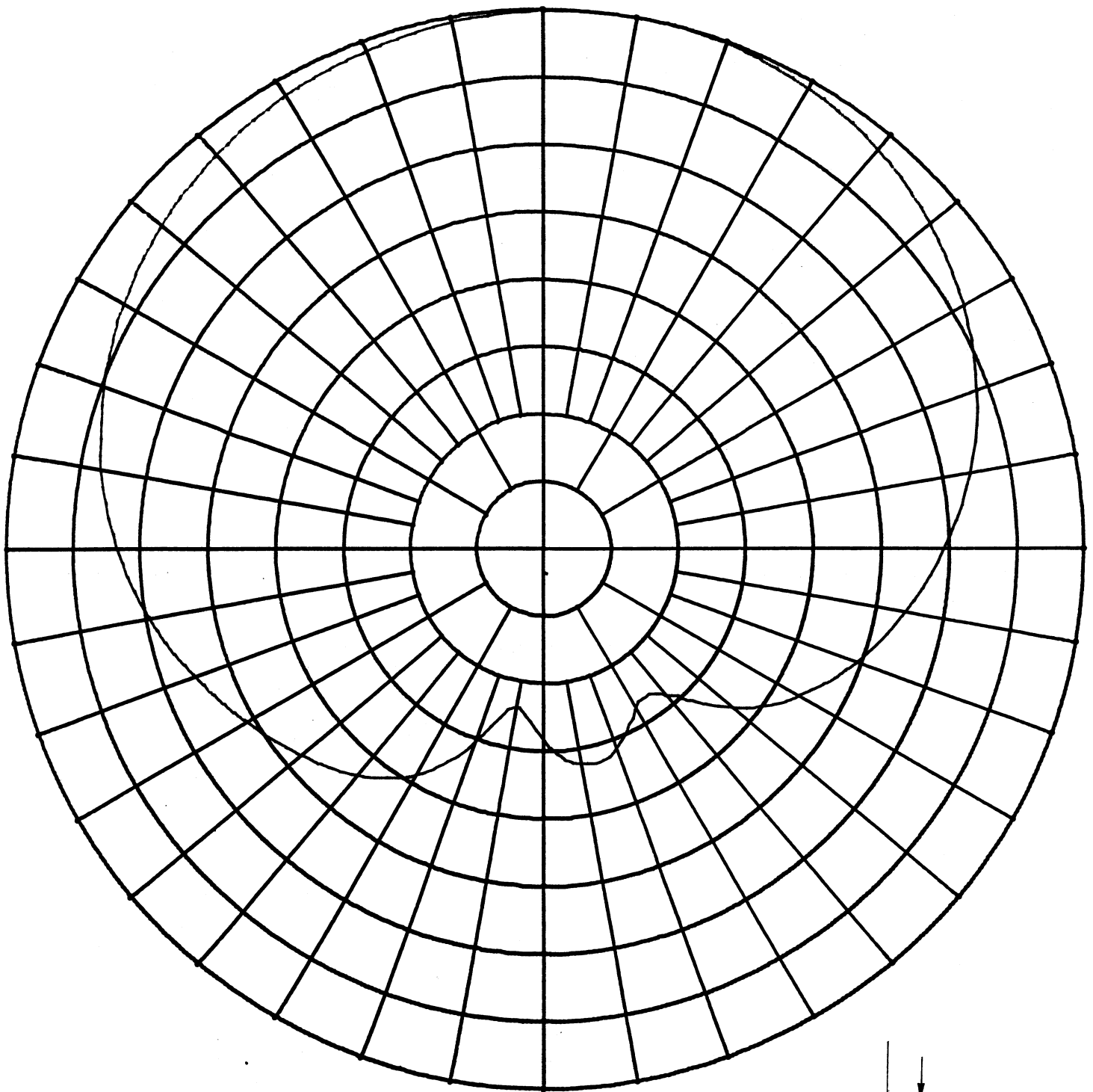
The special rays are derived from the astigmatic wave. If $\rho_1 = \rho_2$, then we have a spherical wave which can be referenced to the caustic.

$$E(d) = E_0 e^{-jk d} \frac{\rho}{(\rho + d)} \quad \text{Spherical Wave}$$

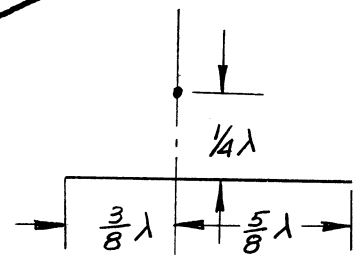
Cylindrical waves are when ρ_1 or ρ_2 is infinite.

$$E(d) = E_0 e^{-jk d} \sqrt{\frac{\rho}{(\rho + d)}} \quad \text{Cylindrical Wave}$$

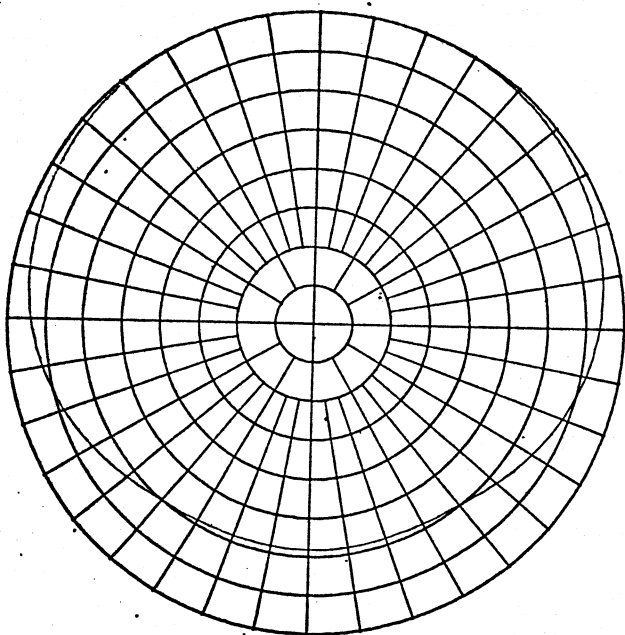
H Plane of Dipole over Ground Plane



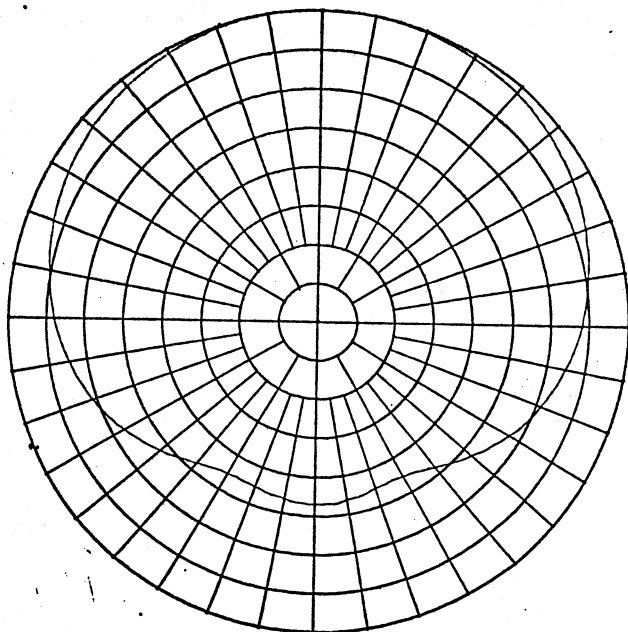
712



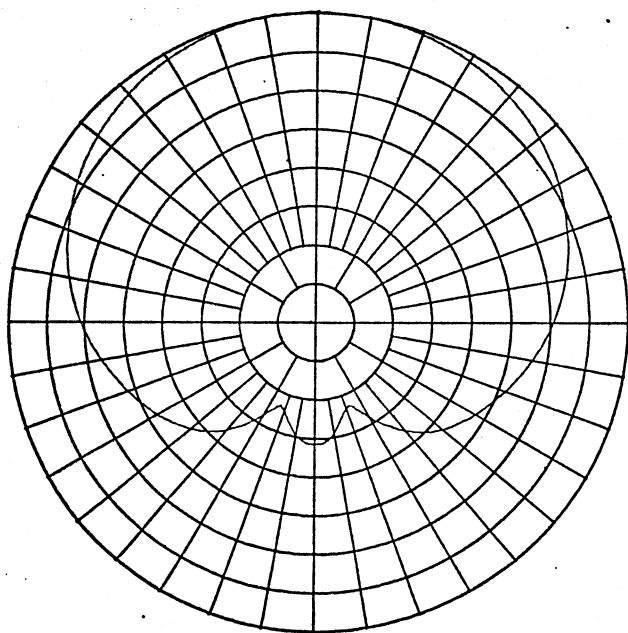
$\lambda/4$ Ground Plane



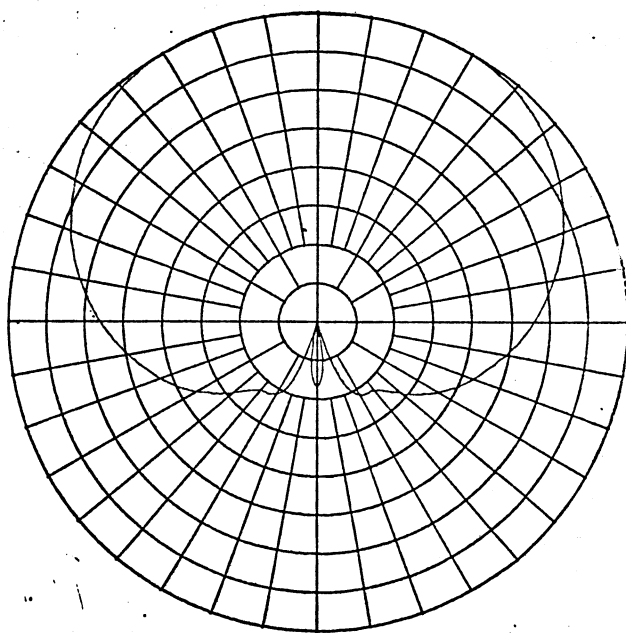
$\lambda/2$ Ground Plane



λ Ground Plane



2λ Ground Plane



H Plane of Dipole over Finite Ground Plane

Plane waves occur when $\rho_1 = \rho_2 = \infty$. $E(d) = E_0 e^{-j k d}$

Both cylindrical and plane waves are nonphysical but are useful approximations. We can solve many problems in two dimensions using cylindrical waves; as was done for the dipole over a ground plane. We use these wave functions for all the direct radiations and the for propagation along all rays. At each interface the radii of curvature have the potential of changing which must be worked through each reflection and diffraction.

REFLECTIONS

When a ray is incident on a surface, the incident ray, the reflected ray, and the normal to the surface at the point of reflection all lie in the same plane with equal angles from the normal to the two rays. We assume that locally the surface acts like a plane surface. Let us look at polarization. The incident wave polarization will be changed, in general, after reflection; for example, right hand circular to left hand circular. The polarization vector is defined in 3 space which means we will need a 3×3 matrix for the transformation of each of the two components. This can be reduced to a 2×2 matrix with only two non-zero if we express the polarization in terms of the ray. Polarization is defined in a plane whose normal is the axis of the ray (pp. 54).

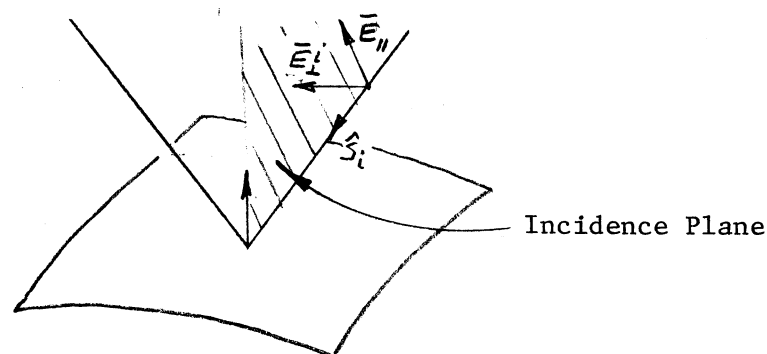
Consider the plane defined by the incident ray and the normal of the surface. We will define two orthogonal unit vectors normal to the incident ray. These vectors as a pair can be orientated at any angle about the ray. We will pick one of these polarization vectors to be in the incident plane, $\bar{a}_{||}^i$, and the other perpendicular, \bar{a}_{\perp}^i . The incident ray is expressed:

$$\bar{E}_i = \bar{a}_{||}^i E_{i||} + \bar{a}_{\perp}^i E_{i\perp}$$

Each component is the projection of the incident ray polarization on to the unit vector.

$$E_{i||}^i = \bar{a}_{||}^i \cdot \bar{E}_i, \text{ etc.}$$

$$\bar{a}_{\perp}^i \times \hat{S}_i = \bar{a}_{||}^i$$

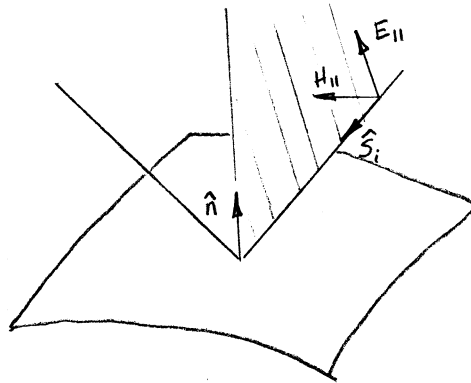


The tangential component, $E_{i\perp}$, is tangent to the surface. From the boundary conditions (pp. 153) we know that the electric field vanishes on the surface

of a conductor. $E_{||}^r = -E_{||}^i$

The reflected wave must cancel the incident wave at the surface. This component will be normal to a plane defined by the normal and the reflected ray. Of course, in the case of a reflection the incident and reflected planes are the same.

The parallel component is at an oblique angle to the surface. We can find the reflection by considering the magnetic field which will be tangent to the surface.



The magnetic field lies along the \bar{a}_{\perp} axis.

$$H_{||}^i \bar{a}_{\perp}^i = \hat{S}_i \times E_{||}^i \bar{a}_{||}^i$$

This tangential magnetic field will induce currents on the surface and reflect phase (pp. 154).

$$H_{||}^i = H_{||}^r$$

The parallel component of the magnetic field does not change direction on reflection but the electric field must.

The reflected ray coordinate system is centered about the ray direction similar to the incident ray. E_{\perp}^r is perpendicular to the reflection plane and since the reflection and incident planes are the same:

$$\bar{a}_{\perp}^r = \bar{a}_{\perp}^i$$

The parallel component in the reflection plane is found from the cross product:

$$\bar{a}_{||}^r = \bar{a}_{\perp}^r \times \bar{S}_r$$

Using these ray centered coordinate systems which are aligned with the incident plane, we can express the reflection in matrix notation.

$$\bar{E}^r(0) = \bar{E}_0^i \cdot \bar{R}$$

\bar{R} is a dyadic (tensor): $\bar{R} = \bar{a}_{||}^i \bar{a}_{||}^r - \bar{a}_{\perp}^i \bar{a}_{\perp}^r$

The reflection is found from carrying out the indicated scalar products.

If we write the reflection in terms of the ray fixed coordinates of the incident and reflected rays, the reflection in matrix terms becomes

$$\begin{bmatrix} E_{\parallel}^r(0) \\ E_{\perp}^r(0) \end{bmatrix} = \begin{bmatrix} 1 & 0 \\ 0 & -1 \end{bmatrix} \begin{bmatrix} E_{\parallel}^i(Q_r) \\ E_{\perp}^i(Q_r) \end{bmatrix}$$

where Q_r is the point of reflection along the incident ray. Of course, the direction of the unit vector \underline{a}_{\perp} changes after reflection.

The total field along the reflected ray is given by

$$\bar{E}_r(s) = \bar{E}_{i_0} \cdot \bar{R} \sqrt{\frac{\rho_1^r \rho_2^r}{(\rho_1^r + s)(\rho_2^r + s)}} e^{-j'ks}$$

s is the distance along the ray and ρ_1, ρ_2 are the reflected ray radii of curvature. For a flat surface we can use images of the incident ray caustics for the centers of curvature. The general curved surface changes both the principle radii of curvature and the orientation of the principle planes relative to the reflected ray centered coordinates. These are given by the expressions:

$$\frac{1}{\rho_1^r} = \frac{1}{2} \left(\frac{1}{\rho_1^i} + \frac{1}{\rho_2^i} \right) + \frac{1}{f_1}$$

$$\frac{1}{\rho_2^r} = \frac{1}{2} \left(\frac{1}{\rho_1^i} + \frac{1}{\rho_2^i} \right) + \frac{1}{f_2}$$

f_1 and f_2 are generalized focal lengths of the surface.

Kouyoumjian and Pathak have derived formulas for the focal lengths of a surface and the direction of the reflected ray principle planes. Suppose we have a reflection on a surface with principle radii of curvature: R_1 and R_2 . The directions of the principle axes are given by unit vectors \bar{u}_1 and \bar{u}_2 . In the ray fixed coordinate system the incident ray will have radii of curvature ρ_1^i and ρ_2^i which are along the orthogonal axes defined by unit vectors: \bar{x}_1^i and \bar{x}_2^i . These vectors are perpendicular to the incident ray. We define a matrix relation between the incident ray principle curvature directions and the surface.

$$\theta = \begin{bmatrix} \bar{x}_1^i \cdot \bar{u}_1 & \bar{x}_1^i \cdot \bar{u}_2 \\ \bar{x}_2^i \cdot \bar{u}_1 & \bar{x}_2^i \cdot \bar{u}_2 \end{bmatrix}$$

The determinant of this matrix is $|\theta| = (\bar{x}_1^i \cdot \bar{u}_1)(\bar{x}_2^i \cdot \bar{u}_2) - (\bar{x}_2^i \cdot \bar{u}_1)(\bar{x}_1^i \cdot \bar{u}_2)$

Kouyoumjian and Pathak, "The Dyadic Diffraction Coefficient for a Curved Edge", NASA CR-2401, June 1974.

Given the angle of incidence (surface normal to incident ray), θ^i , the following are the focal lengths.

$$\begin{aligned} \frac{1}{f_1} &= \frac{\cos \theta^i}{|\theta|^2} \left(\frac{(\theta_{22})^2 + (\theta_{12})^2}{R_1} + \frac{(\theta_{21})^2 + (\theta_{11})^2}{R_2} \right) \\ &\pm \left(\left(\frac{1}{\rho_1^i} - \frac{1}{\rho_2^i} \right)^2 + \left(\frac{1}{\rho_1^i} - \frac{1}{\rho_2^i} \right) \frac{4 \cos \theta^i}{|\theta|^2} \left(\frac{(\theta_{22})^2 - (\theta_{12})^2}{R_1} + \frac{(\theta_{21})^2 - (\theta_{11})^2}{R_2} \right) \right. \\ &\quad \left. \frac{4 \cos^2 \theta^i}{|\theta|^4} \left(\left(\frac{(\theta_{22})^2 + (\theta_{12})^2}{R_1} + \frac{(\theta_{21})^2 + (\theta_{11})^2}{R_2} \right)^2 - \frac{4}{R_1 R_2} \right) \right)^{\frac{1}{2}} \end{aligned}$$

If we only had a single reflection off a surface, it would not be necessary to find the direction of the principle axes. Only the magnitudes of the radii of curvature are needed to find the amplitude variation along the ray. But if there are multiple reflections, then we must also find the directions of the reflected ray principle axes.

To find the reflection principle axes, we must define the following matrices. The incident ray radii of curvature is given by

$$Q_o^i = \begin{bmatrix} \frac{1}{\rho_1^i} & 0 \\ 0 & \frac{1}{\rho_2^i} \end{bmatrix} \quad z = (x_1, x_2) Q_o^i \begin{bmatrix} x_1 \\ x_2 \end{bmatrix}$$

Similiarly, the reflector surface is described by the matrix

$$C_o = \begin{bmatrix} \frac{1}{R_1} & 0 \\ 0 & \frac{1}{R_2} \end{bmatrix}$$

The curvature matrix for the reflected ray is

$$Q^r = Q_o^i + 2 (\theta^{-1})^T C_o \theta^{-1} \cos \theta^i$$

This matrix was diagonalized to find the focal lengths of the reflected ray. We can use the vector reflection formula between incident and reflected rays on the principle axes of the incident ray.

$$\frac{\bar{b}_1^r}{2} = \frac{\bar{x}_1^i}{2} - 2 \left(\bar{n} \cdot \frac{\bar{x}_1^i}{2} \right) \bar{n}$$

The vectors; \bar{b}_1^r and \bar{b}_2^r are not the principle axes of the reflected ray. One of them is found from the formula

$$\bar{\chi}_1^r = \frac{\left[\left(Q_{22}^r - \frac{1}{\rho_1^r} \right) \bar{b}_1^r - Q_{12}^r \bar{b}_2^r \right]}{\sqrt{\left(Q_{22}^r - \frac{1}{\rho_1^r} \right)^2 + \left(Q_{12}^r \right)^2}}$$

The other can be found by the cross product between the reflected ray unit vector and the one principle axis vector, $\bar{\chi}_1^r$.

$$\bar{\chi}_2^r = -\bar{S}^r \times \bar{\chi}_1^r$$

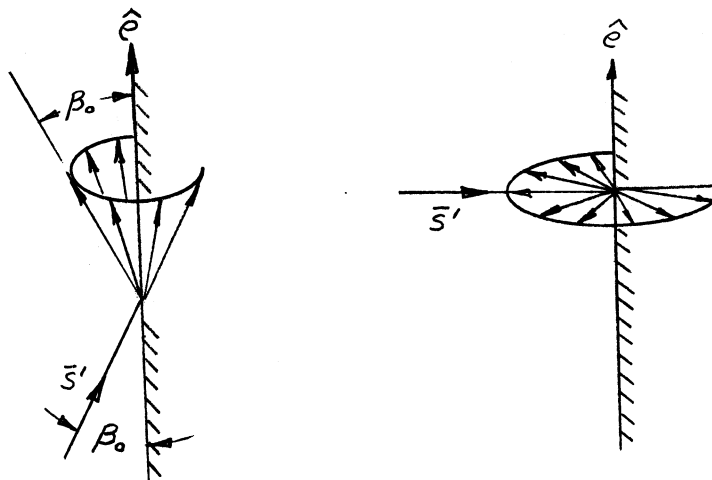
These principle axes vectors must be used with a second reflection to find the new matrix: θ .

With these equations for the reflected wave principle radii of curvature and axes, the geometric optics reflections can be traced through. Remember that the principle axes are not the same as the \parallel and \perp components associated with the reflection matrix and the plane of incidence.

GTD is derived from two canonical problems. These are ones with exact solutions which are matched to over some region of space. The first one is diffraction from a semi-infinite ground plane. This is used to find the diffraction from a wedge. The second canonical problem is the infinite circular cylinder. Creeping wave approximations are matched to this solution. Of course, we will deal with finite objects, but we still assume that locally the wave diffraction is the same as the infinite case.

EDGE DIFFRACTION

J. B. Keller has extended the idea of reflections to edge diffractions. If a ray is incident on an edge, the diffracted rays will form a cone from the point of incidence with the cone angle equal to the incident angle.



The incident angle is measured between the ray and the unit vector tangent to the edge at incidence. In the case of normal incidence, the diffracted rays and the incident ray lie in the same plane. The example of the dipole over a ground plane was handled in two dimensions because there was only normal

incidence and all the diffracted rays remained in the same plane.

The diffraction coefficients are simplified if they are given in terms of incident and diffraction planes. This is an extension of the development for reflected rays. The incidence plane is defined by the cross product of the edge tangent and the incident ray.

$$\bar{a}_{\phi'} = \bar{e} \times \bar{S}' / \sin \beta_0$$

$\bar{a}_{\phi'}$ is the normal to the incident plane, \bar{S}' is the incident ray unit vector. β_0 is the angle between \bar{e} and \bar{S}' . The wave will be diffracted in a cone with the angle between the diffracted ray and the edge tangent also β_0 . There is no unique direction of the diffracted ray except that it lies in the cone. When we pick a particular direction on the cone for the diffracted ray, then we can define a diffraction plane. It is defined by the cross product of the edge tangent vector and the diffracted ray.

$$\bar{a}_{\phi} = -\bar{e} \times \bar{S} / \sin \beta_0$$

\bar{a}_{ϕ} is the normal to the diffraction plane. \bar{S} is the diffracted ray unit vector. We have the following vector relations for diffraction.

$$|\bar{e} \times \bar{S}| = |\bar{e} \times \bar{S}'|$$

$$\bar{e} \cdot \bar{S} = \bar{e} \cdot \bar{S}'$$

These are similar to the laws of reflection (pp. 584) except that the planes are no longer the same and the edge tangent vector is used instead of the surface normal.

We will describe the incident and diffracted wave polarization in terms of parallel and perpendicular components relative to the two planes similar to reflected rays. The perpendicular component is $\bar{a}_{\phi'}$ or \bar{a}_{ϕ} and the parallel component $\bar{a}_{\beta'}$ or \bar{a}_{β_0} . These are ray fixed coordinates.

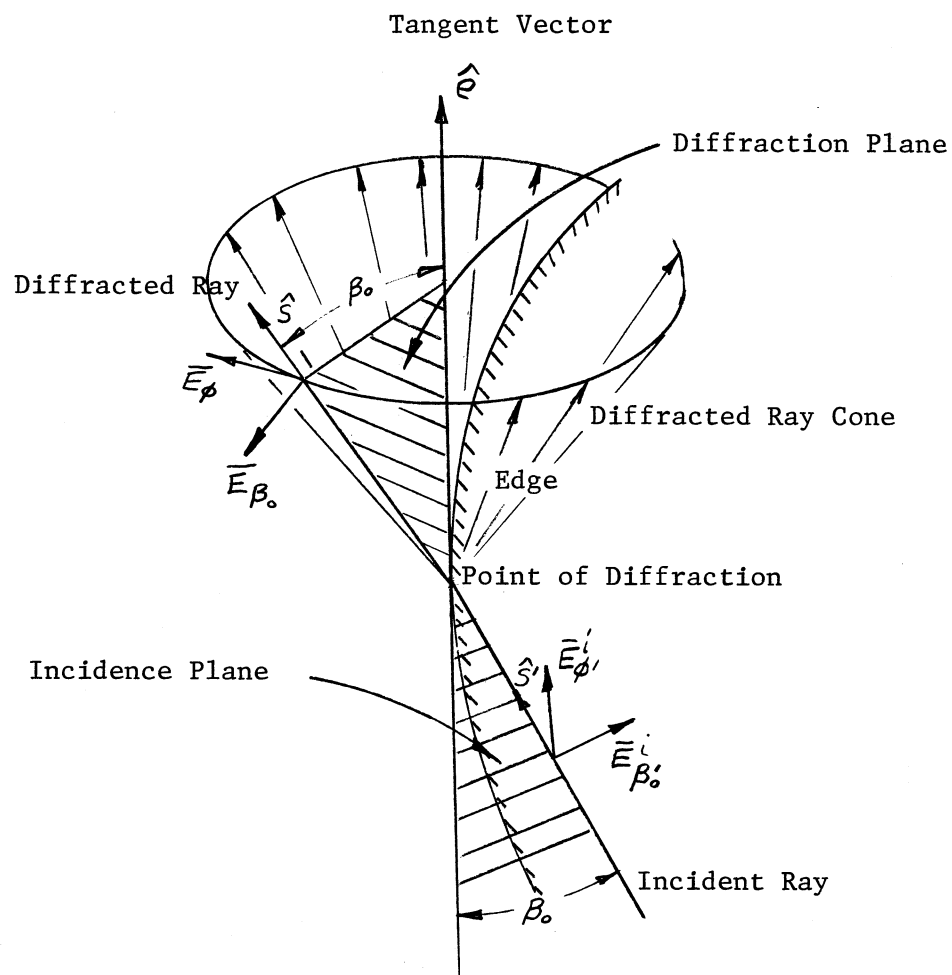
$$\bar{a}_{\phi'} \times \bar{a}_{\beta_0'} = \hat{S}'$$

$$\bar{a}_{\phi} \times \bar{a}_{\beta_0} = \hat{S}$$

The coordinates of the diffraction are drawn on page 720. The incident plane is between the incident ray and the edge tangent. The diffraction plane is between the diffracted ray and the edge tangent. In the case of reflected rays, the two perpendicular unit vectors were the same, but not so for diffractions. This is an extension. Edge diffraction is described by a 2 x 2 matrix with only two non-zero terms.

Consider the case when $\beta_0 = \pi/2$; the two dimensional case. The parallel components of the incident and diffracted rays are parallel to the edge. The electric field must vanish at the edge.

$$\bar{E}_{\beta_0'} + \bar{E}_{\beta_0} = 0$$



Edge Diffraction Incidence and Diffraction Planes

This is Dirichlet boundary conditions. If the edge is along the Z axis, then $E_z = 0$. For acoustic problems this is called the soft boundary condition. We can derive fields which are TM to this edge by satisfying the boundary conditions on E_z . In our case E_{β_0} is the same as E_z .

When we consider the perpendicular component, we repeat the development of reflected rays and consider the magnetic field associated with E_{ϕ} . It is parallel to the edge. This field must satisfy the Neumann boundary condition:

$$\frac{\partial H_z}{\partial n} = 0$$

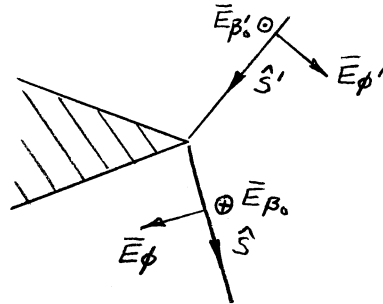
n is normal to the boundary. For acoustic problems this is called the hard boundary condition. The fields derived from H_z are TE waves to the edge.

The diffraction coefficients are derived for these two dimensional fields.

Soft (Dirichlet)	E_z	$E_z = 0$	TM Waves to Z
Hard (Neumann)	H_z	$\frac{\partial H_z}{\partial n} = 0$	TE Waves to Z

In two dimensions the Z components along the edge must satisfy the Helmholtz equation.

$$(\nabla^2 + k^2) \begin{Bmatrix} E_z \\ H_z \end{Bmatrix} = 0$$



If in the diagram of the incident and diffraction planes we let $\beta_0 = 90^\circ$, then we get the above diagram which shows the polarization unit vectors. We assume Z is out of the paper. The general incident ray is given as

$$E_z^i = E^i \sin \beta_0 \quad H_z^i = \frac{E_{\phi}^i}{\eta} \sin \beta_0$$

The two dimensional diffraction is found from the E_z and H_z components.

$$\begin{Bmatrix} E_z^d \\ H_z^d \end{Bmatrix} = \begin{Bmatrix} E_z^i D_s \\ H_z^i D_h \end{Bmatrix} \sqrt{\frac{\rho}{s(\rho+s)}} e^{-jks}$$

The diffracted rays are proportional to the incident fields, a diffraction coefficient (D_s or D_h), and a caustic spreading factor:

$$\sqrt{\frac{\rho}{s(\rho+s)}}$$

S is the distance from the edge to the field point along the diffracted ray. The edge is one of the caustics of the diffracted ray; ρ is the other. The phase is determined by $-kS$.

When we refer to the drawing on page 721 above, we can relate the \bar{a}_{β_0} and \bar{a}_{\emptyset} components to the diffracted fields.

$$E_z^d = -E_{\beta_0}^d \sin \beta_0 \quad H_z^d = -\frac{E_{\phi}^d}{\gamma} \sin \beta_0$$

We can see that the diffracted rays are in opposite direction to the Z components when $\beta_0 = \pi/2$. For the general case the diffraction is written:

$$\begin{Bmatrix} E_{\rho_0}^d \\ E_{\phi_0}^d \end{Bmatrix} = - \begin{Bmatrix} E_{\rho_0}^i & D_s \\ E_{\phi_0}^i & D_h \end{Bmatrix} \sqrt{\frac{\rho}{s(\rho+s)}} e^{-jks}$$

Like the reflected ray, we can write this as a dyadic.

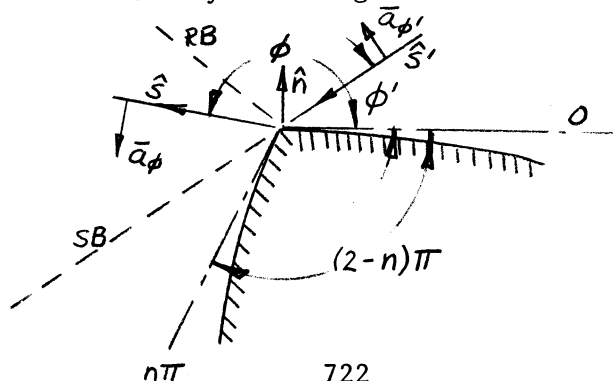
$$\bar{D} = -\bar{a}_{\beta'_0} \bar{a}_{\beta_0} D_s - \bar{a}_{\phi'} \bar{a}_{\phi} D_h$$

In matrix form the diffraction is written:

$$\begin{bmatrix} E_{\beta_0}^d(s) \\ E_{\phi}^d(s) \end{bmatrix} = \begin{bmatrix} -D_s & 0 \\ 0 & -D_n \end{bmatrix} \begin{bmatrix} E_{\beta_0}^i(Q_E) \\ E_{\phi}^i(Q_E) \end{bmatrix} \sqrt{\frac{\rho}{s(s+\rho)}} e^{-jks}$$

We extend the two dimensional diffraction into 3 dimensions by expressing the fields in terms of an incidence plane and a diffraction plane. The two components are either parallel (\underline{a}_{β_0} or \underline{a}_{β_0}) or perpendicular (\underline{a}_{β_1} or \underline{a}_{β_1}) to the planes. There is no component in the direction of incidence (\hat{S}') or diffraction (\hat{S}) because we have assumed that the fields are ray optic (free space electromagnetic waves). To have the diffraction matrix in such simple terms requires coordinate transformations from incident waves which must be aligned with the edge to diffraction waves which are also aligned to a diffraction plane.

Consider a curved wedge cross section at the point of diffraction with the cross section plane defined by the tangent vector.



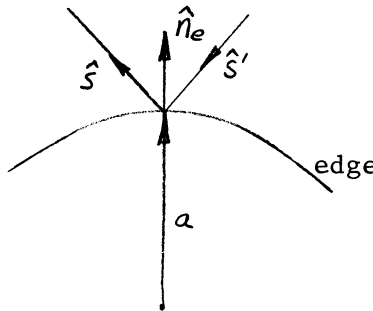
The diffractions are limited by the surfaces 0 and $n\pi$. Waves between this boundary and the surface are creeping waves which are considered separately. These surfaces define an equivalent wedge. The direction of the incident ray is specified by the angles β'_0 and ϕ' . The angle ϕ' is measured from surface 0. The diffraction is also measured from this surface. The wedge angle is $(2 - n)\pi$.

For a given angle of incidence, ϕ' , space around the wedge is divided into 3 regions as shown above. Region I has direct, reflected, and diffracted rays. Region II has direct and diffracted rays; and region III in the shadow has only diffracted rays. If $\phi' \geq (n - 1)\pi$ and $\phi' < \pi$, then there is no shadow boundary and region III is eliminated.

The amplitude of the diffracted ray is determined by the incident ray magnitude at the edge, the diffraction coefficient which is proportional to $1./k^2$, and a spreading factor:

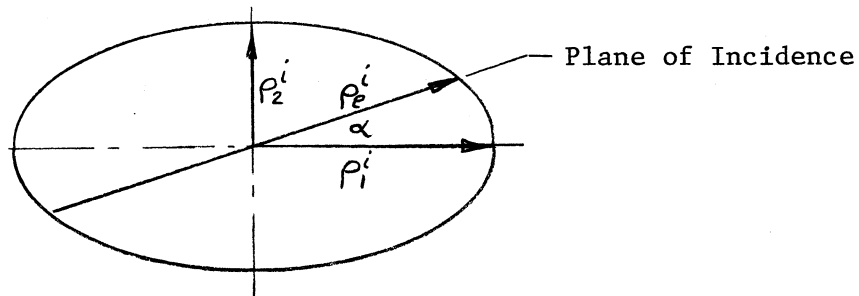
$$\sqrt{\frac{\rho}{s(s+\rho)}}$$

One caustic is at the edge. The second caustic distance, ρ , is determined by the incident ray curvature and the edge curvature.



$$\frac{1}{\rho} = \frac{1}{\rho_e^i} + \frac{1}{f} = \frac{1}{\rho_e^i} - \frac{\hat{n}_e \cdot (\hat{s}' - \hat{s})}{a \sin^2 \beta_0}$$

ρ_e^i is the radius of curvature of the incident ray in the plane of incidence. We can plot the radius of curvature in polar coordinates.



The principle axes have been aligned with the X and Y coordinates. The radius of curvature varies in an ellipse between the principle axes.

$$\rho_e^i = \rho_1^i \cos \alpha + \rho_2^i \sin \alpha$$

The focal length, f , is determined by the edge.

$$1/f = - \frac{\hat{n}_e \cdot (\hat{S}' - \hat{S})}{a \sin^2 \beta_0}$$

a is the radius of curvature of the edge with the direction from the center defined by the unit vector \hat{n}_e . $(\hat{S}' - \hat{S})$ is the difference between the incident and diffracted rays. β_0 is the angle between the edge tangent and the incident (and diffracted) ray.

If the edge is straight at the point of diffraction, $a \rightarrow \infty$ and $1/f = 0$. The caustic distance of the diffracted ray is determined by the incident ray curvature in the incidence plane.

WEDGE DIFFRACTION COEFFICIENTS

The wedge diffraction coefficients were first formulated by J. B. Keller. His diffraction coefficient is:

$$D_s = \frac{e^{-j\pi/4} \sin \frac{\pi}{n}}{n \sqrt{2\pi k} \sin \beta_0} \left[\frac{1}{\cos \frac{\pi}{n} - \cos \left(\frac{\phi - \phi'}{n} \right)} + \frac{1}{\cos \frac{\pi}{n} - \cos \left(\frac{\phi + \phi'}{n} \right)} \right]$$

Remember that D_s is the soft diffraction coefficient which is used with Dirichlet boundary conditions ($E_z = 0$, TM) and D_h , the hard diffraction coefficient, is used with Neumann boundary conditions ($\partial H_z / \partial n = 0$, TE). The units of the diffraction coefficient is $\lambda^{1/2}$. Wedge diffraction is weaker than the incident and reflected rays by this factor. As the frequency increases, the diffraction coefficient decreases. This is not true, however, at the shadow and reflection boundaries.

Consider the term: $\cos \frac{\pi}{n} - \cos \left(\frac{\phi - \phi'}{n} \right)$

As the diffracted ray direction approaches the shadow boundary, $\phi \rightarrow \phi' + \pi$, the difference of cosines approaches zero, and the first term in the brackets approaches infinity. Likewise, when we consider the second term:

$$\cos \frac{\pi}{n} - \cos \left(\frac{\phi' + \phi}{n} \right)$$

this term approaches zero and the diffraction coefficient infinity when ϕ , the diffracted ray direction, approaches the reflection boundary. The diffraction coefficient gives good results provided the diffracted ray is not too close to these boundaries.

Because the diffraction coefficients at the shadow and reflection boundaries were infinite, GTD was not extensively used. This problem was solved by R. G. Kouyoumjian and P. H. Pathak who expanded the field at these boundaries in an asymptotic expansion and forced continuity. This is called the uniform theory of diffraction. Their wedge diffraction coefficient is given as:

$$D_{sh} = \frac{-e^{-j\pi/4}}{2n\sqrt{2\pi k} \sin \beta_o} \left[\cot\left(\frac{\pi + (\phi - \phi')}{2n}\right) F(k L^i a^+(\phi - \phi')) \right. \\ \left. + \cot\left(\frac{\pi - (\phi - \phi')}{2n}\right) F(k L^i a^-(\phi - \phi')) \right. \\ \left. + \left(\cot\left(\frac{\pi + (\phi + \phi')}{2n}\right) F(k L^{rn} a^+(\phi + \phi')) + \right. \right. \\ \left. \left. \cot\left(\frac{\pi - (\phi + \phi')}{2n}\right) F(k L^{ro} a^-(\phi + \phi')) \right) \right]$$

In short hand this is written: $D_{sh} = D(1) + D(2) + (D(3) + D(4))$

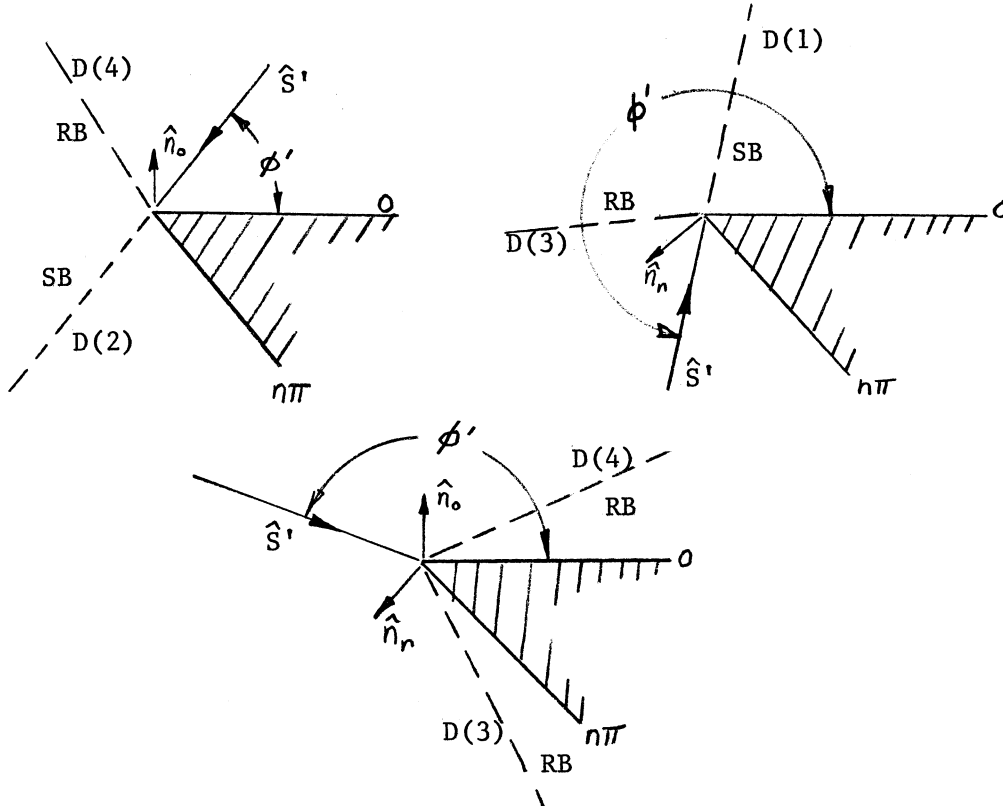
The first two terms are associated with the shadow boundary because they provide for a smooth transition across them. The second two terms are associated with the reflection boundary. Consider the cotangent factors, they are singular when the argument is zero.

$$D(1) \quad \frac{\pi + (\phi - \phi')}{2n} = 0 \quad \phi = \phi' - \pi, \text{ SB, surface 0 is shadowed}$$

$$D(2) \quad \frac{\pi - (\phi - \phi')}{2n} = 0 \quad \phi = \phi' + \pi, \text{ SB, Surface } n\pi \text{ is shadowed}$$

$$D(3) \quad \frac{\pi + (\phi + \phi')}{2n} = 0 \quad \phi = (2n - 1)\pi - \phi', \text{ Reflection from surface } n\pi$$

$$D(4) \quad \frac{\pi - (\phi + \phi')}{2n} = 0 \quad \phi = \pi - \phi', \text{ Reflection from surface 0}$$



Above are the three possible types of incident rays. When the diffracted ray is near one of the transition boundaries (SB or RB), then that term will dominate the diffraction coefficient. We will continue to associate each portion of the diffraction coefficient with its transition boundary.

The diffraction coefficient is not infinite at the transition boundaries because the cotangent is multiplied by the transition function, $F(x)$.

$$F(x) = 2j\sqrt{x} e^{jx} \int_{\sqrt{x}}^{\infty} e^{-j\tau^2} d\tau$$

This is the form of a Fresnel integral. The function varies between 0 and 1, and approaches zero as x approaches zero. For large arguments it is one. The magnitude and phase are plotted on page 727.

$$a^{\pm}(\phi \pm \phi') = 2 \cos^2((2n\pi N^{\pm} - (\phi \pm \phi'))/2)$$

in which N^{\pm} are integers which most nearly satisfy the equations

$$2\pi n N^{+} - (\phi \pm \phi') = \pi$$

and

$$2\pi n N^{-} - (\phi \pm \phi') = -\pi$$

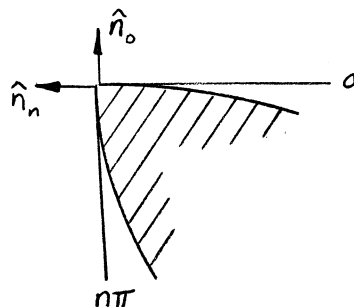
The terms L^i , L^{ro} , and L^{rn} are distance parameters which are determined by the requirement of continuity across the various transition boundaries (SB or RB).

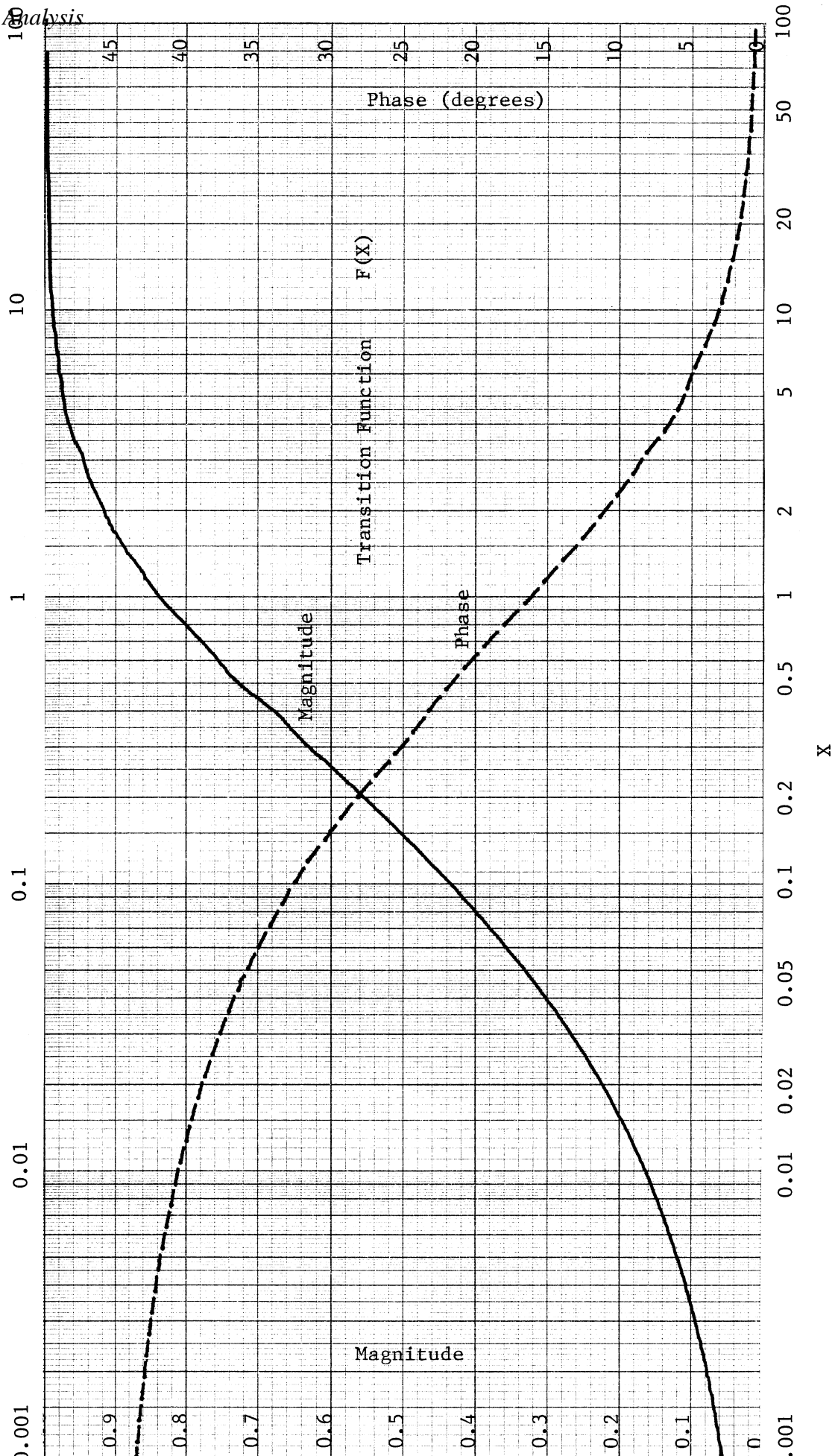
L^i is associated with the shadow boundary.

$$L^i = \frac{s(\rho_e^i + s)\rho_1^i \rho_2^i \sin^2 \beta_0}{\rho_e^i(\rho_1^i + s)(\rho_2^i + s)}$$

ρ_1^i and ρ_2^i are the principle radii of curvature of the incident ray. ρ_e^i is the radius of curvature in the incident plane. s is the distance from the diffraction point to the far field point.

Consider a curved edge as shown below. The edge has a curvature a with the direction from the center of curvature given by \hat{n}_e .





There are two normals to the planes 0 and n at the edge; \hat{n}_0 and \hat{n}_n . The reflection boundaries are with respect to these normals. For waves reflected off these surfaces, the radii of curvature will be changed. The distance parameters, L^r , are associated with each of these sides.

$$L^{ro} = \frac{s(\rho_e^{ro} + s) \rho_1^{ro} \rho_2^{ro} \sin^2 \beta_0}{\rho_e^{ro} (\rho_1^{ro} + s) (\rho_2^{ro} + s)}$$

$$L^{rn} = \frac{s(\rho_e^{rn} + s) \rho_1^{rn} \rho_2^{rn} \sin^2 \beta_0}{\rho_e^{rn} (\rho_1^{rn} + s) (\rho_2^{rn} + s)}$$

ρ_1^{ro} and ρ_2^{ro} are the principle radii of curvature of the wave reflected from surface 0.

ρ_1^{rn} and ρ_2^{rn} are the principle radii of curvature of the wave reflected from surface n.

$$\frac{1}{\rho_e^{ro}} = \frac{1}{\rho_e^i} - \frac{2(\hat{n}_0 \cdot \hat{n}_e)(\hat{S}' \cdot \hat{n}_0)}{a \sin^2 \beta_0}$$

$$\frac{1}{\rho_e^{rn}} = \frac{1}{\rho_e^i} - \frac{2(\hat{n}_n \cdot \hat{n}_e)(\hat{S}' \cdot \hat{n}_n)}{a \sin^2 \beta_0}$$

We have the general case which will simplified for various special cases.

Far Field: $s \rightarrow \infty$

$$L^i = \frac{\rho_1^i \rho_2^i \sin^2 \beta_0}{\rho_e^i} \quad L^{ro} = \frac{\rho_1^{ro} \rho_2^{ro} \sin^2 \beta_0}{\rho_e^{ro}} \quad L^n = \frac{\rho_1^{rn} \rho_2^{rn} \sin^2 \beta_0}{\rho_e^{rn}}$$

Spherical Wave Incident, General: $\rho_1^i = \rho_2^i = \rho_e^i = s'$

$$L^i = \frac{s s' \sin^2 \beta_0}{s + s'} \quad L^{ro} = \frac{s(\rho_e^{ro} + s) \rho_1^{ro} \rho_2^{ro} \sin^2 \beta_0}{\rho_e^{ro} (\rho_1^{ro} + s) (\rho_2^{ro} + s)}$$

$$L^{rn} = \frac{s(\rho_e^{rn} + s) \rho_1^{rn} \rho_2^{rn} \sin^2 \beta_0}{\rho_e^{rn} (\rho_1^{rn} + s) (\rho_2^{rn} + s)}$$

Plane Wave Incident: $\rho_1^i = \rho_2^i = \rho_e^i \rightarrow \infty$

$$L^i = s \sin^2 \beta_0 \quad L^{ro} \text{ \& } L^{rn} \text{ are the same as before}$$

If we are in the far field, L^i approaches infinity and the transition function approaches one. But we are also at the caustic of the incident wave and cannot expect the field to be accurately predicted.

Spherical Wave Incident, Far Field:

$$L^i = s' \sin^2 \beta_0 \quad L^{ro} = \frac{\rho_1^{ro} \rho_2^{ro} \sin^2 \beta_0}{\rho_e^{ro}}$$

$$L^{rn} = \frac{\rho_1^{rn} \rho_2^{rn} \sin^2 \beta_0}{\rho_e^{rn}}$$

Straight Edge: $a \rightarrow \infty \quad \frac{1}{\rho_e^{ro}} = \frac{1}{\rho_e^{rn}} = \frac{1}{\rho_e^i}$

$$L^i = \frac{s(\rho_e^i + s) \rho_1^i \rho_2^i \sin^2 \beta_0}{\rho_e^i (\rho_1^i + s) (\rho_2^i + s)}$$

$$L^{ro} = \frac{s(\rho_e^i + s) \rho_1^{ro} \rho_2^{ro} \sin^2 \beta_0}{\rho_e^i (\rho_1^{ro} + s) (\rho_2^{ro} + s)} \quad L^{rn} = \frac{s(\rho_e^i + s) \rho_1^{rn} \rho_2^{rn} \sin^2 \beta_0}{\rho_e^i (\rho_1^{rn} + s) (\rho_2^{rn} + s)}$$

Not much has changed because ρ_1^{ro} , ρ_2^{ro} , ρ_1^{rn} , and ρ_2^{rn} depend on the local edge radii of curvature of the two faces.

Straight Edge, Spherical Wave Incident: $\rho_e^i = s'$

$$L^i = \frac{ss' \sin^2 \beta_0}{s + s'} \quad L^{ro} = \frac{s(s' + s) \rho_1^{ro} \rho_2^{ro} \sin^2 \beta_0}{s'(\rho_1^{ro} + s) (\rho_2^{ro} + s)} \quad L^{rn} = \frac{s(s' + s) \rho_1^{rn} \rho_2^{rn} \sin^2 \beta_0}{s'(\rho_1^{rn} + s) (\rho_2^{rn} + s)}$$

Straight Edge, Cylindrical Wave Incident: $\rho_2^i \rightarrow \infty \quad \beta_0 = 90^\circ \quad \rho_1^i = s'$

$$\rho_e^i \rightarrow \infty \quad \rho_2^{ro} \rightarrow \infty \quad \rho_2^{rn} \rightarrow \infty$$

$$L^i = \frac{ss'}{s + s'} \quad L^{ro} = \frac{s \rho_1^{ro}}{\rho_1^{ro} + s} \quad L^{rn} = \frac{s \rho_1^{rn}}{\rho_1^{rn} + s}$$

Far Field

$$L^i = s' \quad L^{ro} = \rho_1^{ro} \quad L^{rn} = \rho_1^{rn}$$

Wedge with Plane Sides

The reflected rays will have the same radii of curvature as the incident ray.

$$\rho_1^{\text{ro}} = \rho_1^{\text{rn}} = \rho_1^{\text{i}} \quad \rho_2^{\text{ro}} = \rho_2^{\text{rn}} = \rho_2^{\text{i}}$$

$$L^{\text{i}} = \frac{s(\rho_e^{\text{i}} + s) \rho_1^{\text{i}} \rho_2^{\text{i}} \sin^2 \beta_0}{\rho_e^{\text{i}} (\rho_1^{\text{i}} + s) (\rho_2^{\text{i}} + s)}$$

$$L^{\text{ro}} = \frac{s(\rho_e^{\text{ro}} + s) \rho_1^{\text{i}} \rho_2^{\text{i}} \sin^2 \beta_0}{\rho_e^{\text{ro}} (\rho_1^{\text{i}} + s) (\rho_2^{\text{i}} + s)} \quad L^{\text{rn}} = \frac{s(\rho_e^{\text{rn}} + s) \rho_1^{\text{i}} \rho_2^{\text{i}} \sin^2 \beta_0}{\rho_e^{\text{rn}} (\rho_1^{\text{i}} + s) (\rho_2^{\text{i}} + s)}$$

We still have ρ_e^{ro} and ρ_e^{rn} because the wedge may have a curved edge.

Wedge with Plane Sides, Spherical Wave Incident

$$L^{\text{i}} = \frac{ss'}{s+s'} \sin^2 \beta_0 \quad L^{\text{ro}} = \frac{s(\rho_e^{\text{ro}} + s) \left(\frac{s' \sin \beta_0}{s' + s} \right)^2}{\rho_e^{\text{ro}}}$$

$$L^{\text{rn}} = \frac{s(\rho_e^{\text{rn}} + s) \left(\frac{s' \sin \beta_0}{s' + s} \right)^2}{\rho_e^{\text{rn}}}$$

Wedge with Plane Sides and Straight Edge

The reflected rays will have the same curvature as the incident ray and the curvature in the diffracted plane is the same as the incident plane since a (the curvature of the edge) approaches infinity.

$$L^{\text{i}} = L^{\text{ro}} = L^{\text{rn}} = L$$

$$L = \frac{s(\rho_e^{\text{i}} + s) \rho_1^{\text{i}} \rho_2^{\text{i}} \sin^2 \beta_0}{\rho_e^{\text{i}} (\rho_1^{\text{i}} + s) (\rho_2^{\text{i}} + s)}$$

Spherical Wave Incident: $\rho_1^{\text{i}} = \rho_2^{\text{i}} = \rho_e^{\text{i}} = s'$

$$L = \frac{ss'}{s+s'} \sin^2 \beta_0$$

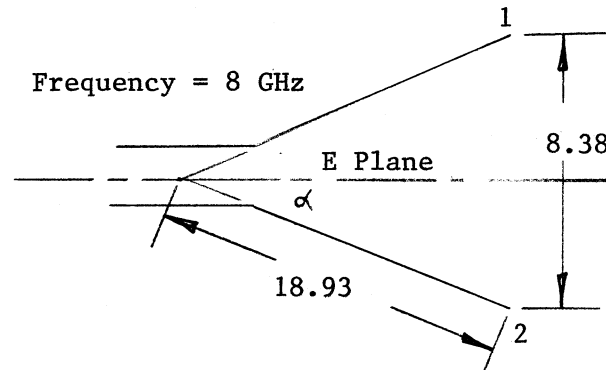
Cylindrical Wave Incident: $\beta_0 = 90^\circ$, $\rho_1^{\text{i}} = s'$, $\rho_2^{\text{i}} = \rho_e^{\text{i}} \rightarrow \infty$

$$L = \frac{ss'}{s+s'}$$

E PLANE ANALYSIS OF A HORN

We will use the problem of finding the E plane pattern of a horn to demonstrate the use of the wedge diffraction coefficient. The problem easily reduces to 2 dimensions because we are only interested in one plane. This also avoids the extensive geometry required for a 3 dimensional solution.

Consider the horn designed on page 224 and analyzed on page 574.



The angle of the sides from the center line is $\tan^{-1}(4.19/18.93) = 12.5^\circ$. We will analyze this by a cylindrical structure with a H_z magnetic line source placed at the vertex. This requires Neumann boundary conditions: $\partial H_z / \partial n = 0$; it gives TE waves and uses hard diffraction coefficients as spelled out on page 721. We discussed the geometric optics fields on page 703. It is bounded by the flare angle of the horn and is a uniform amplitude as shown on page 732.

We have edge diffractions from the termination of the sides. Consider the diffractions from edge 1. These will radiate in all directions except the horn itself will block some of the radiation. If α is the slant angle of the side, then the range of the pattern angle, θ , for diffraction from edge 1 is given by

$$-\pi/2 \leq \theta \leq \pi + \alpha \quad \text{edge 1 diffractions}$$

Similarly, the diffractions from edge 2 will be blocked by the horn.

$$-\pi - \alpha \leq \theta \leq \pi/2 \quad \text{edge 2 diffractions}$$

The diffractions from the edges will be of the form

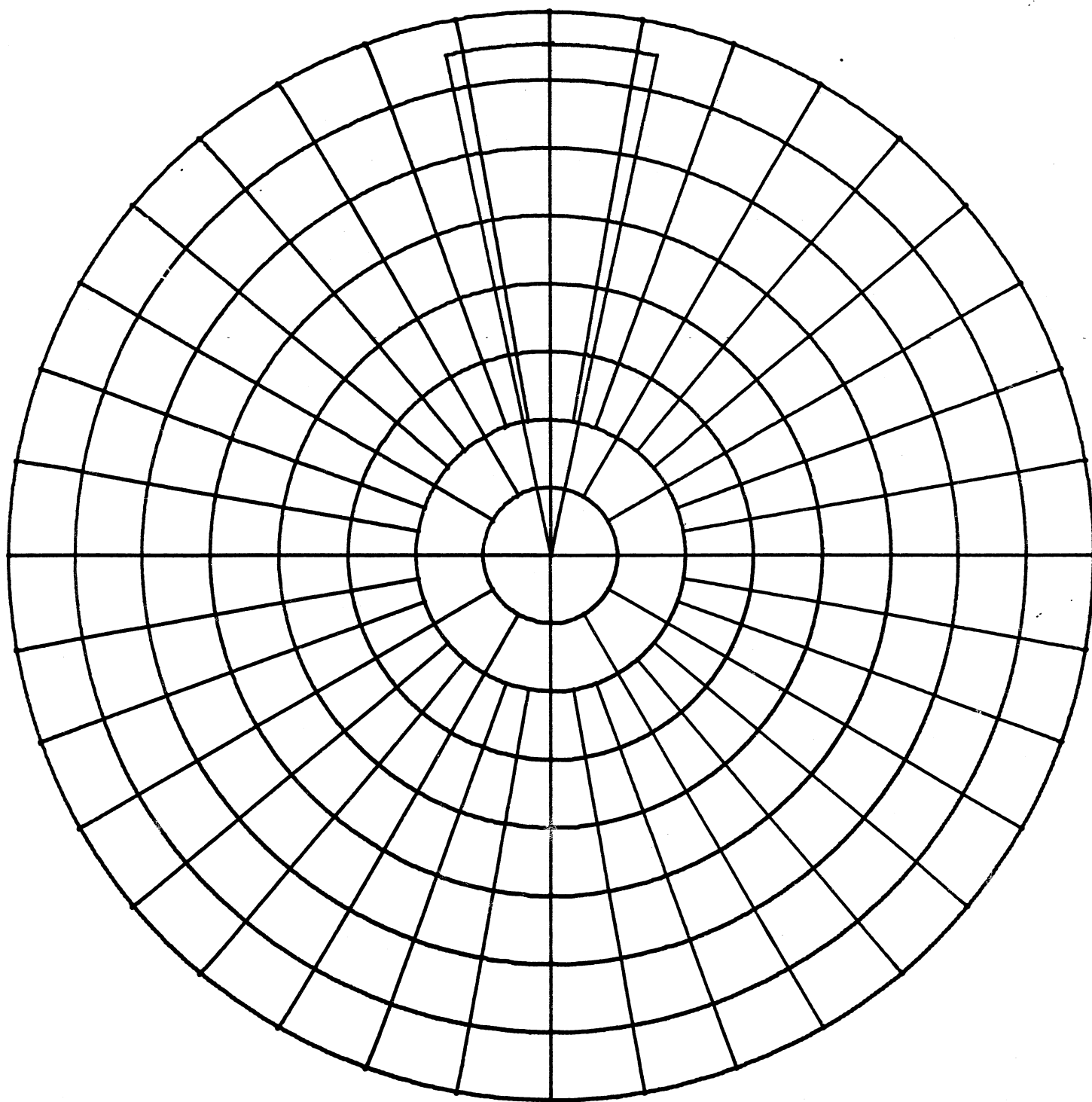
$$H_z^d = H_z^i D_h \sqrt{\frac{\rho}{s(\rho+s)}} e^{-jk s}$$

H_z^i is the incident wave at the edges. Consider both edges; the radius of curvature is infinite, therefore the spreading caustic in the plane of the edge will be the same as the incident wave.

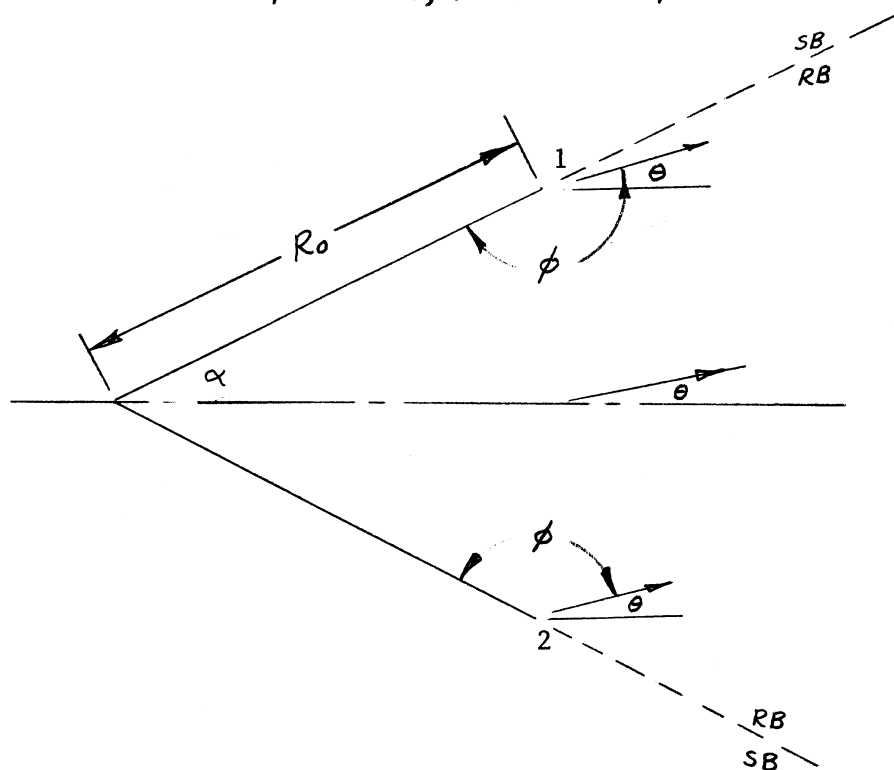
$$1/\rho = 1/\rho_e^i \quad (\text{pp. 723})$$

Since the incident wave is cylindrical, $\rho \rightarrow \infty$ and the spreading factor of the diffractions is $1/\sqrt{S}$ where S is the distance from the edge.

E Plane of Horn; Geometric Optics Field



$$\sqrt{\frac{\rho}{s(\rho+s)}} = \frac{1}{\sqrt{s(1+s/\rho)}} \xrightarrow{\rho \rightarrow \infty} \frac{1}{\sqrt{s}}$$



It is indicated on the drawing above that the shadow and reflection boundaries are the same. We have this because of the grazing incidence on the sides. The geometric optics fields given on page 732 includes both the direct and reflected radiation. In this case we cannot separate the two contributions. We normally do not consider grazing incidence to be reflected, but if we take the limit as the angle between the incident ray and the surface approaches zero, for any angle greater than zero there is a reflected ray. The combination gives the following field.

$$H_z^{GO} = \frac{2 H_{zo}}{\sqrt{R}} e^{-j k R}$$

R is the distance from the virtual apex. The reflected waves have the same caustic distance as the source because the sides are flat. We only consider the incident wave on the edges to be direct from the source and not including the reflected ray. It is convenient to normalize to the sum of the direct and reflected rays.

$$H_z^{GO} = \frac{H_{zo}}{\sqrt{R}} e^{-j k R}$$

The incident ray on the edges is given by

$$H_z^i = H_{zo}/2 \frac{e^{-j k R_o}}{\sqrt{R_o}}$$

R_o is the slant length of the horn. This gives us the diffracted waves.

$$H_z^d = \frac{H_{z0}}{2\sqrt{R_o}} e^{-jkR_o} D_h(L, \phi, \phi', n) \frac{e^{-jks}}{\sqrt{s}}$$

Because the sides are planes, $L^i = L^{ro} = L^{rn} = L$. The distance parameter for cylindrical waves is

$$L = \frac{R_o S}{R_o + S} \quad \text{since } R_o = S'$$

The diffraction coefficient has been written as a function of four parameters. ϕ' , the angle of incidence is zero. The wedge angle constant, n , is two because we assume a thin wall on the horn. The angle ϕ to the field point is measured from the walls of the horn as shown.

$$\text{Edge 1} \quad \phi_1 = \pi - \alpha + \theta$$

$$\text{Edge 2} \quad \phi_2 = \pi - \alpha - \theta$$

Notice that the angles ϕ_1 and ϕ_2 are measured in opposite directions. The amplitudes of the edge diffractions are plotted on page 735. Notice the sharp transitions in the back lobes where the horn shadows the diffractions.

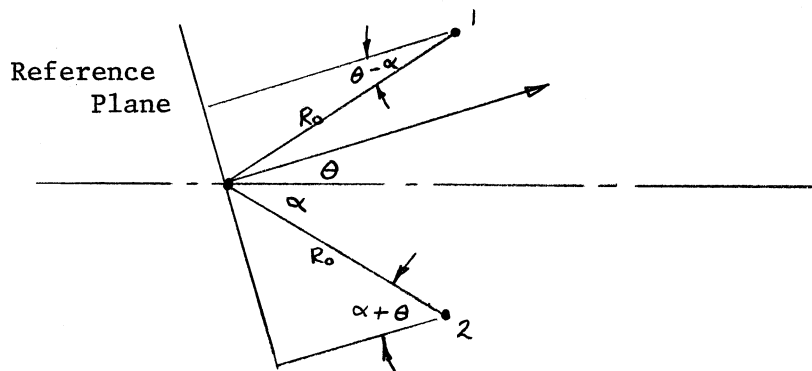
Now we must combine these patterns. First, we will consider only the far field: $S \rightarrow \infty$. We make the usual far field approximation that the differ-

$$L = R_o \quad S = R$$

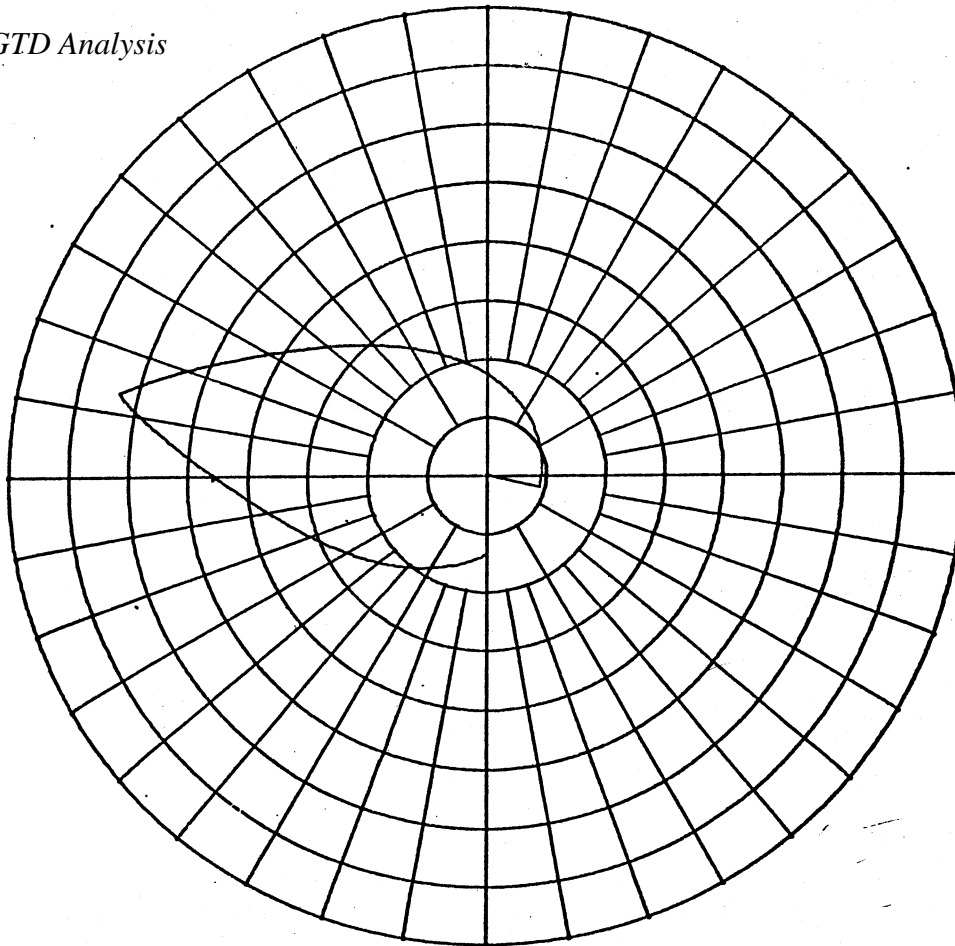
ence in distance has no effect on amplitude and we can separate out the term:

$$\frac{e^{-jkR}}{\sqrt{R}}$$

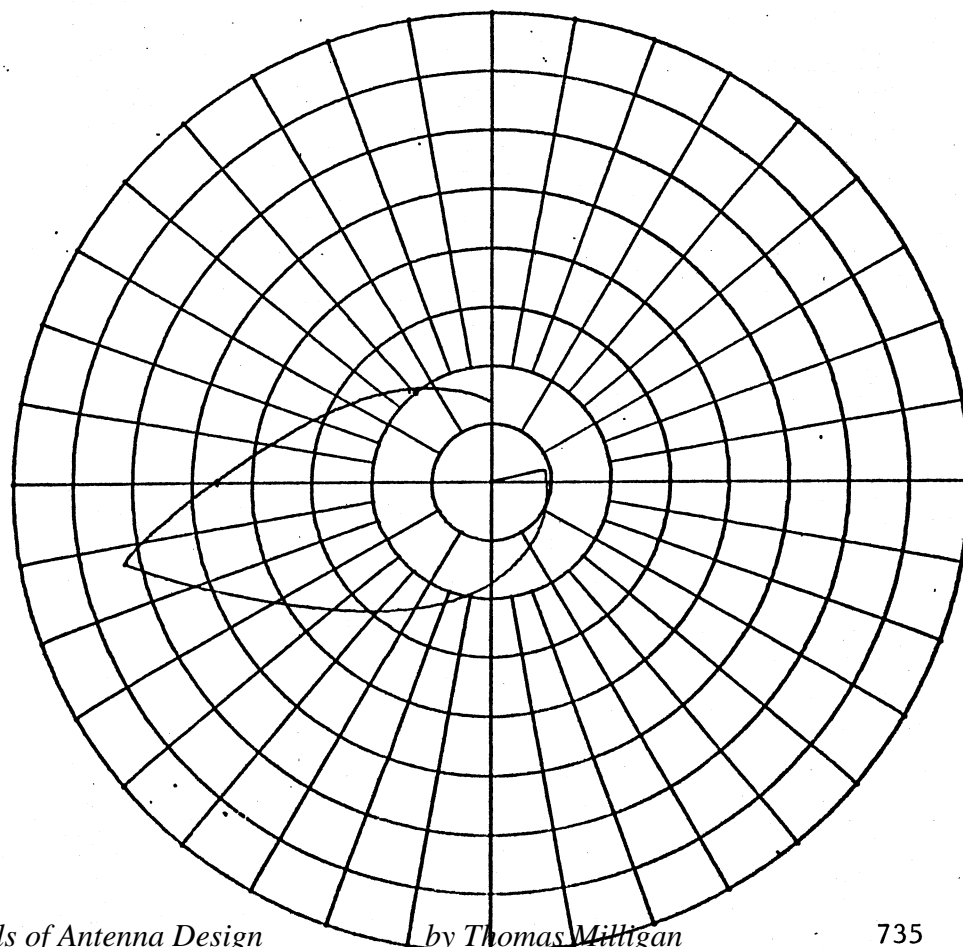
The horn is represented by a three element array. The phase reference point



Edge Diffraction



Edge Diffraction



E Plane Pattern of Horn

is the vertex of the horn. Of course, each element of the array has a different pattern which is determined by the G.O. field or diffraction coefficient. The distance of edge 1 to the reference plane is given by

$$R_o \cos(\theta - \alpha)$$

while the distance of the second edge is $R_o \cos(\theta + \alpha)$

The sum of these three components is

$$H_z = H_{zo} \left(1. + \frac{e^{-j k R_o}}{2 \sqrt{R_o}} D_h(R_o, \pi - \alpha + \theta, 0, 2) e^{j k R_o \cos(\theta - \alpha)} \right. \\ \left. + \frac{e^{-j k R_o}}{2 \sqrt{R_o}} D_h(R_o, \pi - \alpha - \theta, 0, 2) e^{j k R_o \cos(\theta + \alpha)} \right) \frac{e^{-jkR}}{\sqrt{R}}$$

This expression must be applied with restriction on the terms. The first term, 1., represents the G.O. field; it is restricted to the flare angle of the sides. The second term is the diffraction from edge 1; it is shadowed by the horn. The third term is the diffraction from edge 2 and it too is shadowed by the horn. As long as we take into account the restrictions on the terms, the above expression is the fields of the horn.

Using the short hand notation, the diffraction coefficient is the sum of all four terms.

$$D_h = D(1) + D(2) + D(3) + D(4)$$

Because the reflection and shadow boundaries are the same,

$$D(3) = D(1) \quad (\text{surface 0 shadowed})$$

$$D(4) = D(2) \quad (\text{surface } n\pi \text{ shadowed})$$

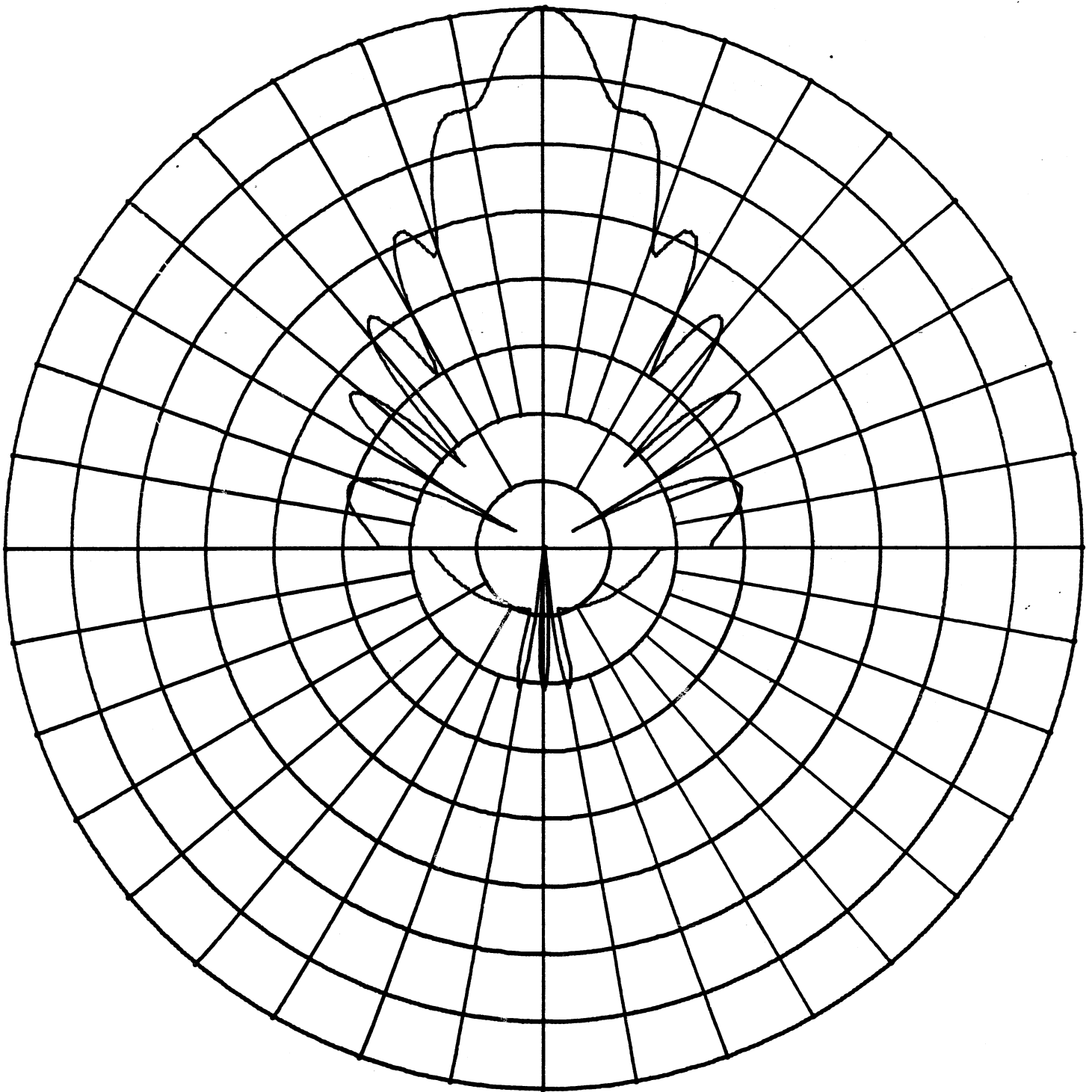
$$D_h = 2(D(1) + D(2))$$

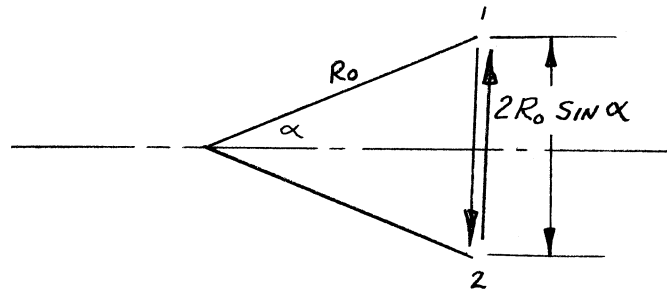
The phasor sum of the expression for the pattern is plotted on page 737. The pattern is good over most of the front lobe and predicts the backlobe. We can notice that there is a discontinuity in the pattern at $\pm 90^\circ$. This means that there is an unaccounted for diffraction which is important in this region. But the inaccuracy has a limited angle variation. In general, this is true of all discontinuities in the patterns found by GTD.

The factor which has not been accounted for is double diffraction. Edge 1 has a diffracted ray in the direction of edge 2 and vice versa. These rays will be diffracted by the second edge.

E Plane Pattern of Horn

G.O. Field + Edge Diffraction





The diffraction between the edges is near field; the distance parameter becomes

$$L = \frac{2 R_o R_o \sin \alpha}{R_o + 2 R_o \sin \alpha} = \frac{2 R_o \sin \alpha}{1 + 2 \sin \alpha}$$

$$\phi' = 0 \quad \phi = \pi/2 - \alpha \quad \text{for both edges.}$$

The incident wave on edge 1 is $H_{zo} \frac{e^{-jkR_o}}{2 \sqrt{R_o}}$

The ray diffracted to edge 2 is

$$H_{12} = H_{zo} \frac{e^{-jkR_o}}{2 \sqrt{R_o}} D_h \left(\frac{2 R_o \sin \alpha}{1 + 2 \sin \alpha}, \pi/2 - \alpha, 0, 2 \right) \frac{e^{-j2kR_o \sin \alpha}}{\sqrt{2 R_o \sin \alpha}}$$

This is the incident wave on edge 2. The diffracted wave is diffracted by edge 2.

$$L = 2 R_o \sin \alpha \quad (\text{far field})$$

$$H_{12}^d = H_{12} D_h(2 R_o \sin \alpha, \pi - \alpha + \theta, \pi/2 - \alpha, 2)$$

As indicated above, the incident wave $H_{21} = H_{12}$ from symmetry and the double diffraction from edge 1 is

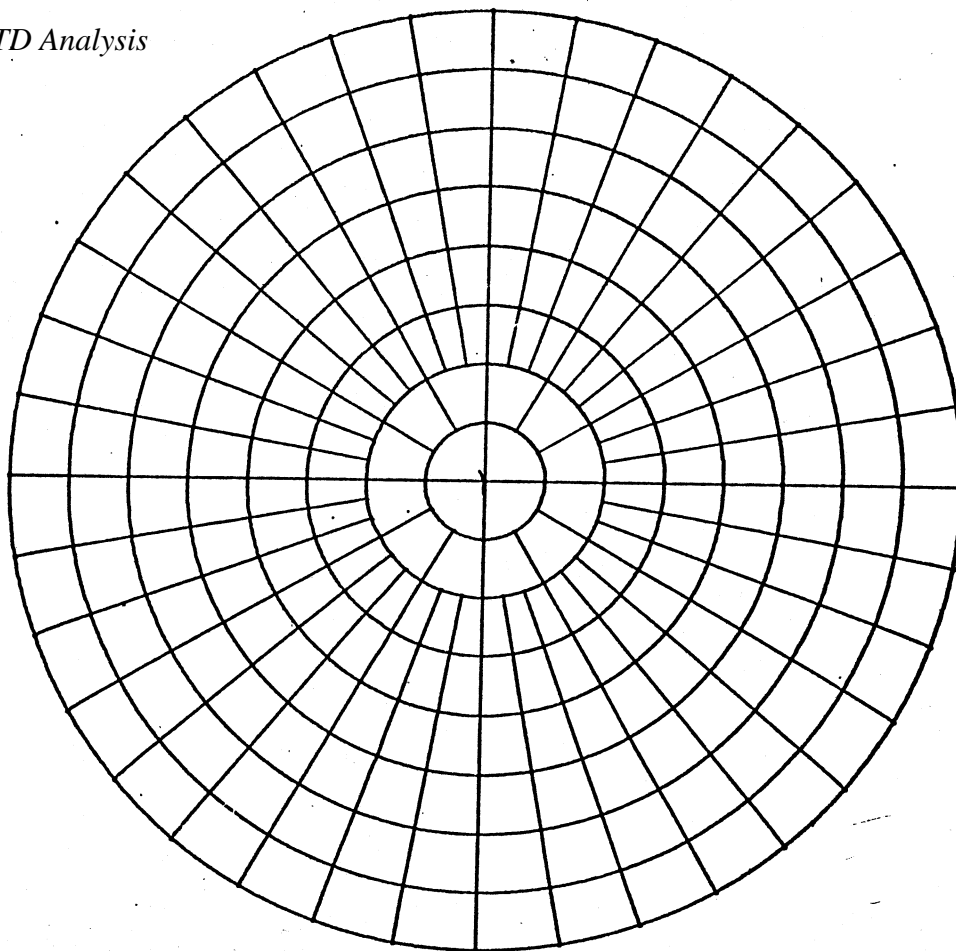
$$H_{21}^d = H_{21} D_h(2 R_o \sin \alpha, \pi - \alpha - \theta, \pi/2 - \alpha, 2)$$

Notice that the angle of incidence, ϕ' , is no longer zero. The magnitude of the double diffractions relative to the total pattern is plotted on page 739.

The double diffraction is a two element array at the edges. The pattern of the double diffraction is given by

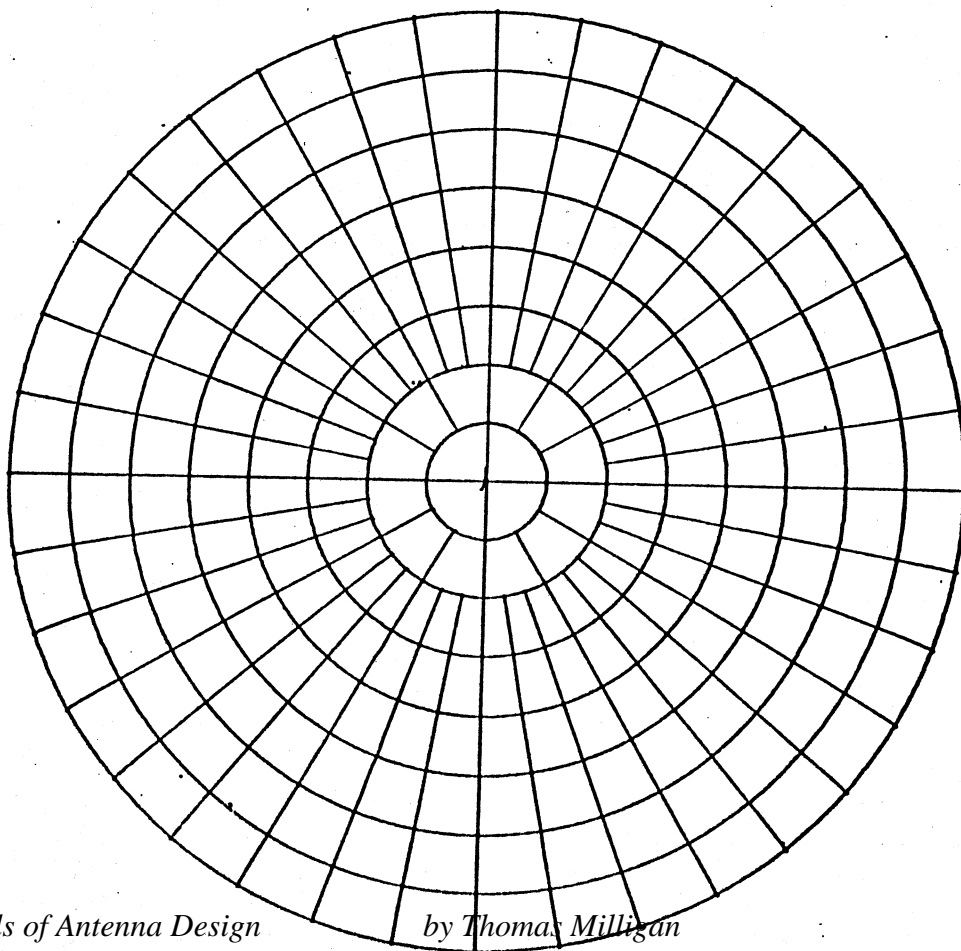
$$\begin{aligned} & H_{zo} \frac{e^{-jkR_o}}{2 \sqrt{R_o}} D_h \left(\frac{2 R_o}{1 + 2 \sin \alpha}, \pi/2 - \alpha, 0 \right) \frac{e^{-jkR_o \sin \alpha}}{\sqrt{2 R_o \sin \alpha}} (\\ & D_h(2 R_o \sin \alpha, \pi - \alpha + \theta, \pi/2 - \alpha) e^{jkR_o \cos(\theta - \alpha)} \\ & + D_h(2 R_o \sin \alpha, \pi - \alpha - \theta, \pi/2 - \alpha) e^{jkR_o \cos(\theta + \alpha)}) \frac{e^{-jkR}}{\sqrt{R}} \end{aligned}$$

Double Edge Diffraction



E Plane Pattern of Horn

Double Edge Diffraction



When this array is added to the pattern on page 737, we get the pattern on page 741. There is still a small discontinuity at $\theta = \pm 90^\circ$, but it is small and only effects one angle.

We can compare the GTD pattern with one found by aperture integration which is plotted on page 742. The general patterns are similar only the sidelobes of the GTD solution are higher. The aperture integration method fails to predict the pattern sidelobes accurately because it was assumed that the fields outside the mouth of the horn are zero. This is not the case. Since GTD has not made any such assumptions, it can accurately predict the pattern.

SLOPE DIFFRACTION

When we consider the H plane pattern of a horn, we find no edge diffracted fields because the incident field vanishes on the slant sides. But the pattern is not the geometric optics field given on page 703. To get an accurate pattern, we must include higher order diffractions. Slope diffraction is a second order diffraction which depends on the space derivative of the incident field.

Slope diffraction is like edge diffraction in that it satisfies Keller's extension of reflection to diffraction (pp. 718). The diffraction is in a cone with its vertex at the point of incidence on the edge. The half angle of the cone with respect to the edge vector equals the angle of the incident ray with respect to the edge. The slope diffraction is defined in terms of the planes of incidence and diffraction as shown on page 720. Slope diffraction is written

$$\begin{bmatrix} E_{\beta_0}^d \\ E_{\phi_0}^d \end{bmatrix} = \begin{bmatrix} -e_s & 0 \\ 0 & -e_h \end{bmatrix} \begin{bmatrix} E_{\beta_0}^i \\ E_{\phi_0}^i \end{bmatrix} \sqrt{\frac{\rho}{s(s+\rho)}} e^{-jks}$$

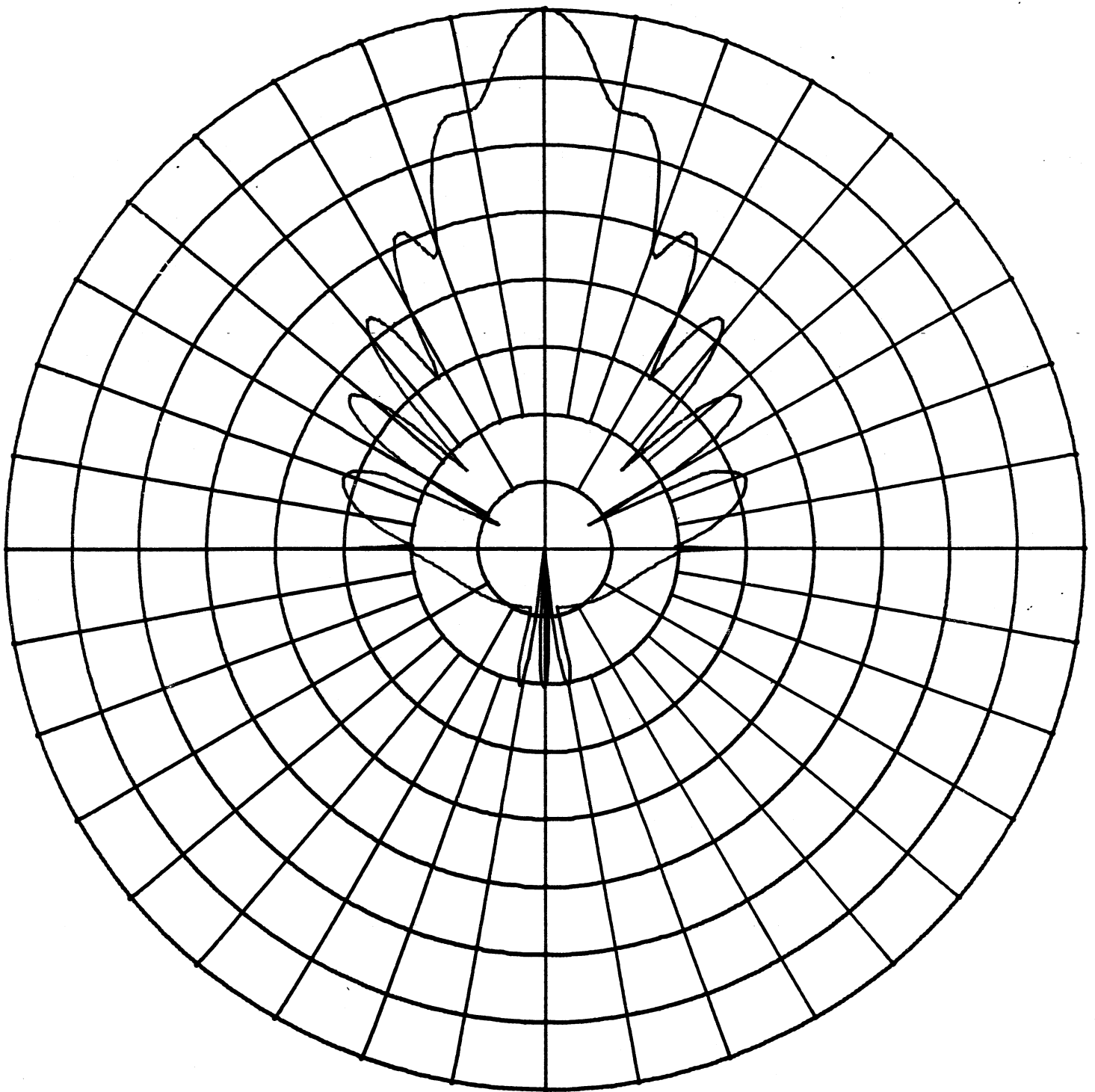
This is the same form as edge diffraction on page 722. One caustic of the diffracted field is on the edge (S). The other, ρ , is given by

$$\frac{1}{\rho} = \frac{1}{\rho_e^i} - \frac{\hat{n}_e \cdot (\hat{S}' - \hat{S})}{a \sin^2 \beta_0}$$

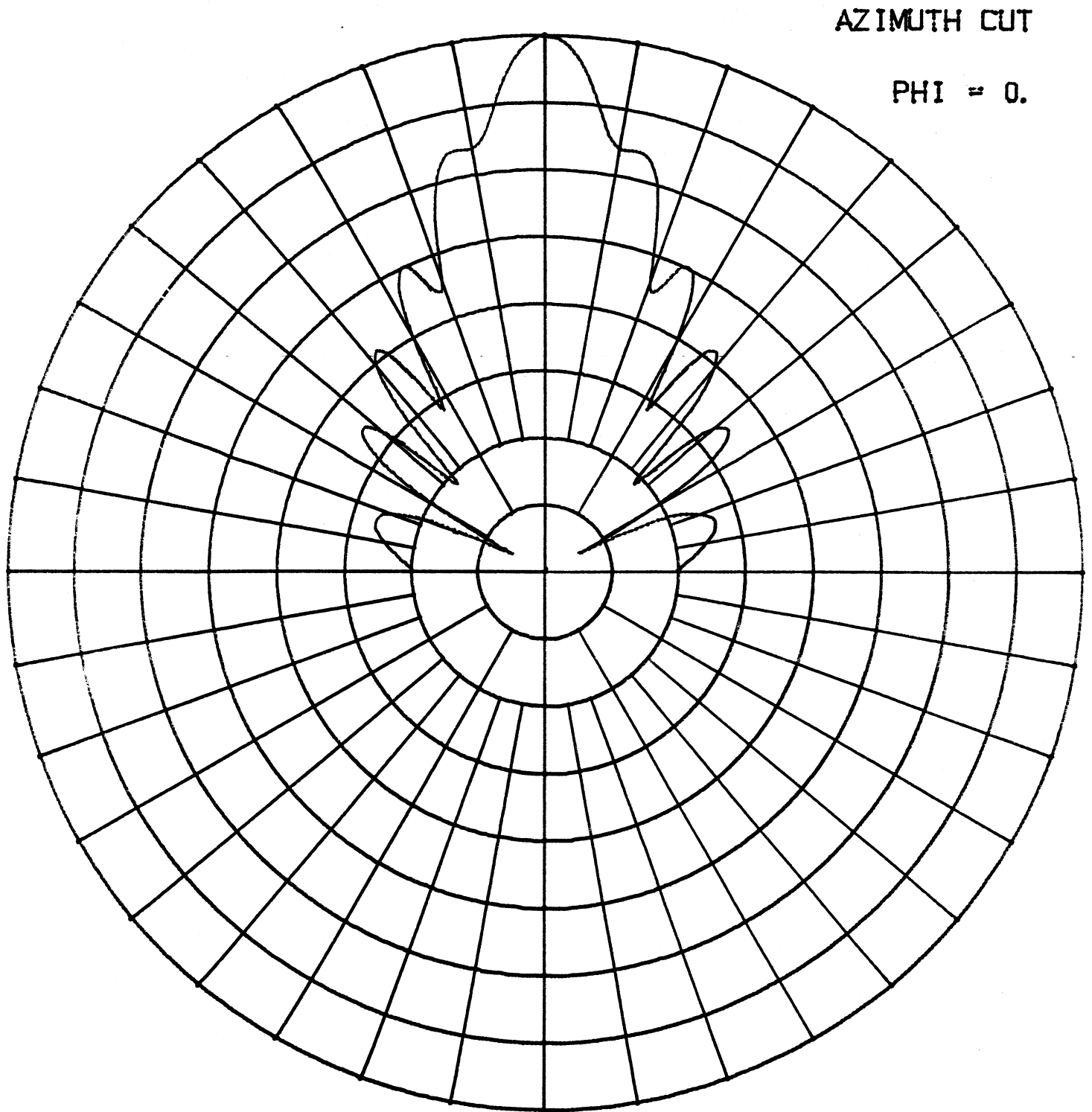
ρ_e^i is the radius of curvature of the incident ray in the incidence plane. a is the radius of curvature of the edge. \hat{n}_e is the unit vector from the center of curvature of the edge to the diffraction point. \hat{S}' is the incident ray unit vector; \hat{S} is the diffracted ray unit vector.

$$e_{s,h} = \frac{1}{jK \sin \beta_0} \left[\frac{\partial D_{s,h}}{\partial \phi'} \frac{\partial}{\partial n'} \right]$$

Total E Plane Pattern of Horn



E Plane Pattern of Horn; using Aperture Integration



$$\left[\frac{\partial D_{s,h}}{\partial \phi'} \frac{\partial E}{\partial n'} \right] = \frac{-e^{-j\pi/4}}{4n^2 \sqrt{2\pi k} \sin^2 \beta_0} \left\{ \left[\csc^2 \left(\frac{\pi + \phi - \phi'}{2n} \right) F_s(k L^i a^+(\phi - \phi')) \right. \right. \\ \left. \left. - \csc^2 \left(\frac{\pi - (\phi - \phi')}{2n} \right) F_s(k L^i a^-(\phi - \phi')) \right] \frac{\partial E^i}{\partial n'} \right. \\ \left. + \left[\csc^2 \left(\frac{\pi + (\phi + \phi')}{2n} \right) F_s(k L^{rn} a^+(\phi + \phi')) \frac{\partial E^{rn}}{\partial n'} \right. \right. \\ \left. \left. - \csc^2 \left(\frac{\pi - (\phi + \phi')}{2n} \right) F_s(k L^{ro} a^-(\phi + \phi')) \frac{\partial E^{ro}}{\partial n'} \right] \right\}$$

The slope diffraction coefficient uses a different transition function.

$$F_s(x) = j 2x + 4x^{3/2} e^{jx} \int_{\sqrt{x}}^{\infty} e^{-j\tau^2} d\tau$$

This is related to the first order edge diffraction transition function.

$$F_s(x) = j 2x (1 - F(x))$$

The functions a^+ and a^- are defined on page 726 along with L^i , L^{ro} , and L^{rn} . L for various special cases are given on pages 728 - 730.

The slope of the incident field $\partial E^i / \partial n'$ is in the direction of the $\bar{a}_{\phi'}$ coordinate. This can be found by a dyadic.

$$\nabla \bar{E}^i$$

The gradient of a vector is a dyadic. The derivative in the direction of $\bar{a}_{\phi'}$ is given by

$$\bar{a}_{\phi'} \cdot \nabla \bar{E}^i = \frac{\partial \bar{E}^i}{\partial n'}$$

In most cases we can ignore the curvature of the edge surfaces, if any, for this secondary diffraction and assume flat plate reflection. As with edge

$$\bar{a}_{\phi'} \cdot \nabla \bar{E}^i = \bar{a}_{\phi'} \cdot \nabla \bar{E}^{ro} = \bar{a}_{\phi'} \cdot \nabla \bar{E}^{rn}$$

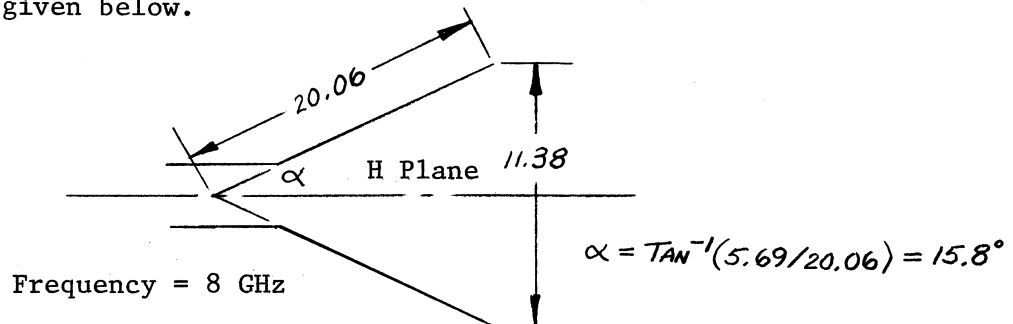
diffraction, each term in the slope diffraction is associated with a shadow or reflection boundary.

$$\left[\frac{\partial D_{s,h}}{\partial \phi'} \right] = D(1) - D(2) + (D(3) - D(4))$$

The various terms, $D(i)$ have the same association as given on page 725 except, of course, these terms are different.

H PLANE ANALYSIS OF A HORN

Slope diffraction is used to find the H plane pattern of a horn. This problem reduces to 2 dimensions and is handled by a cylindrical wedge and cylindrical waves. The dimensions in the H plane of the horn analyzed on page 731 are given below.



We analyze this using an electric line source, E_z , placed at the vertex of the projected sides. The G.O. field of this horn z was given on page 703.

$$E^{GO} = \frac{e^{-jkR}}{\sqrt{R}} \cos\left(\frac{\pi \tan \theta}{2 \tan \alpha}\right)$$

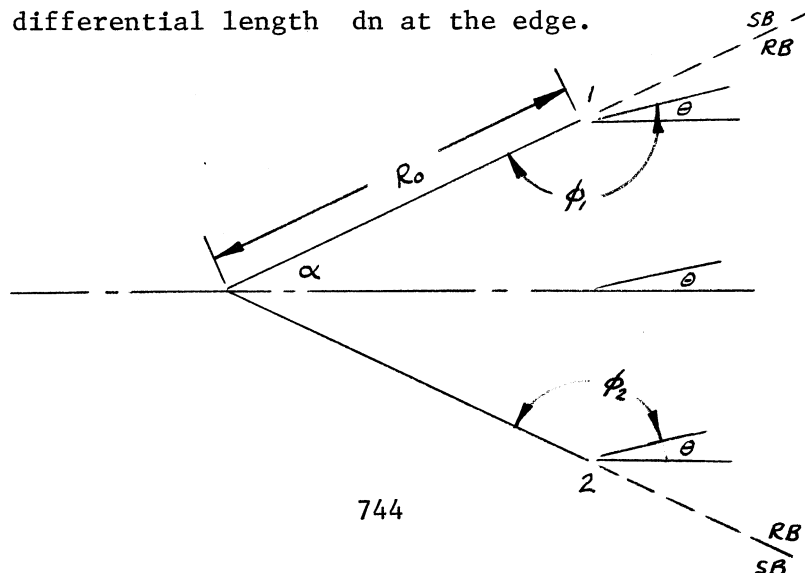
$$E^{GO} = 0 \quad \text{elsewhere}$$

The amplitude of this field is plotted on page 745. We can see that the pattern is zero (-40 dB) beyond $\pm \alpha$ and that it tapers to zero on the edges. Since the incident field is zero at the edges, there is no first order edge diffraction.

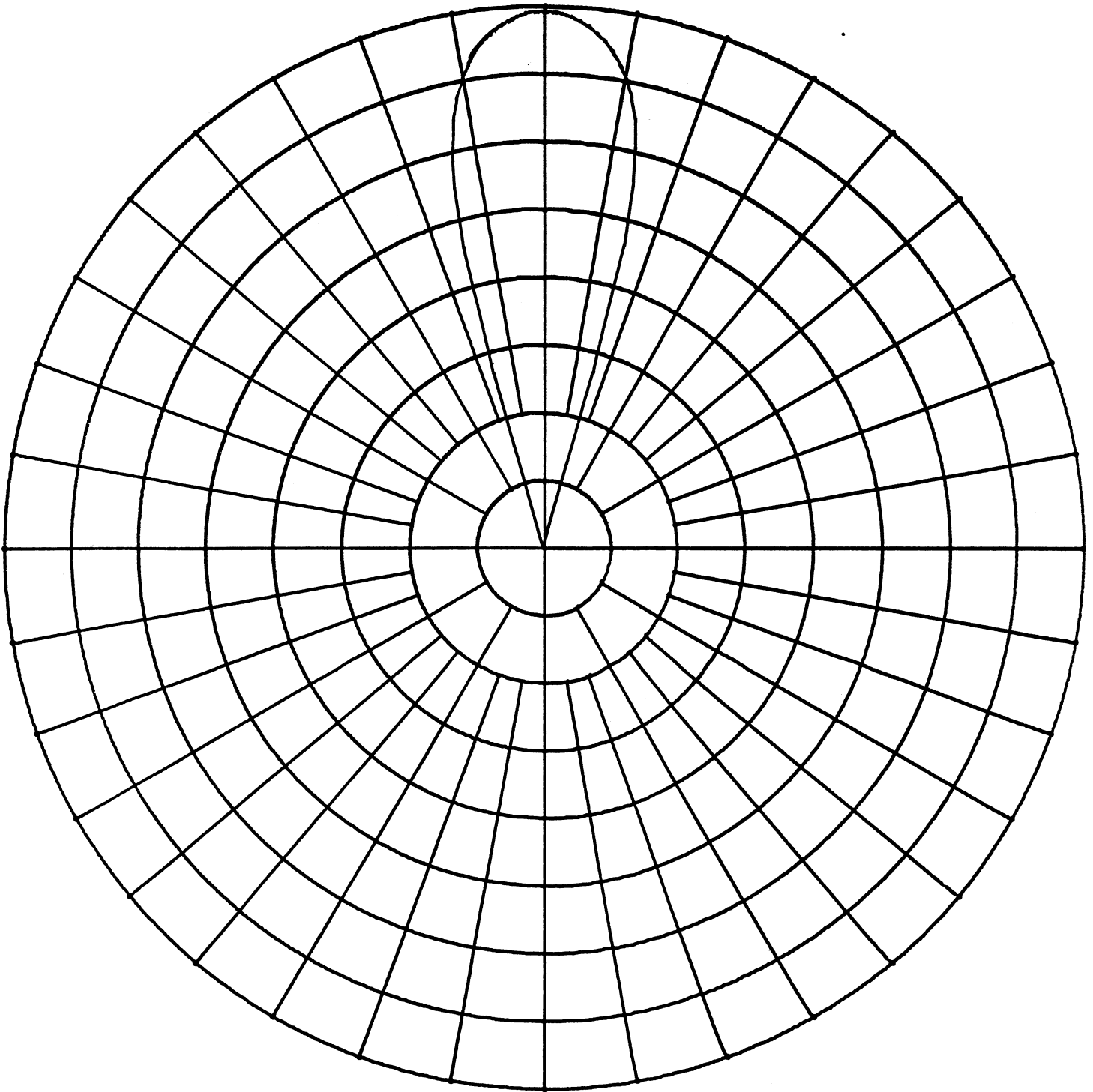
To find the slope diffracted field, we must find the space derivative of the incident field at the edge. The plane of incidence is out of the paper, since the edge tangent is out of the paper. The vector \underline{a}_0 is normal to the surface at grazing incidence.

$$\frac{\partial E^i}{\partial n'} = \frac{1}{R_0} \frac{\partial E^i(R_0)}{\partial \phi'}$$

$R_0 d\theta'$ is the differential length dn at the edge.



H Plane of Horn; Geometric Optics Field



On edge 1 $\partial\phi_1 = -\partial\theta$.

$$\begin{aligned}\frac{\partial E^i}{\partial n} &= -\frac{1}{R_0} \left. \frac{\partial E^i(R_0)}{\partial \theta} \right|_{\theta=\alpha} \\ &= -\frac{e^{-jkR_0}}{\sqrt{R_0} R_0} \left. \frac{\partial}{\partial \theta} \left(\cos \left(\frac{\pi \tan \theta}{2 \tan \alpha} \right) \right) \right|_{\theta=\alpha} \\ &= \frac{e^{-jkR_0} \pi}{R_0^{3/2} \sin(2\alpha)}\end{aligned}$$

We get the same expression on edge 2.

The edge diffractions only occur over a limited region of θ because they are blocked by the horn.

$$-\pi/2 \leq \theta \leq \pi + \alpha \quad \text{edge 1 diffractions}$$

$$-\pi - \alpha \leq \theta \leq \pi/2 \quad \text{edge 2 diffractions}$$

The diffractions from the edges will be of the form.

$$E_z^d = \frac{\partial E_z^i}{\partial n} \frac{\partial D_s}{\partial \phi'} \sqrt{\frac{\rho}{s(\rho+s)}} e^{-jks}$$

The radius of curvature of the edges is infinite ($a \rightarrow \infty$) and the spreading caustic in the plane of the edge is the same as the incident wave which is infinite for cylindrical waves.

$$\sqrt{\frac{\rho}{s(\rho+s)}} = \frac{1}{\sqrt{s}}$$

The soft slope diffraction coefficient is used with the Dirichlet boundary conditions ($E_z = 0$).

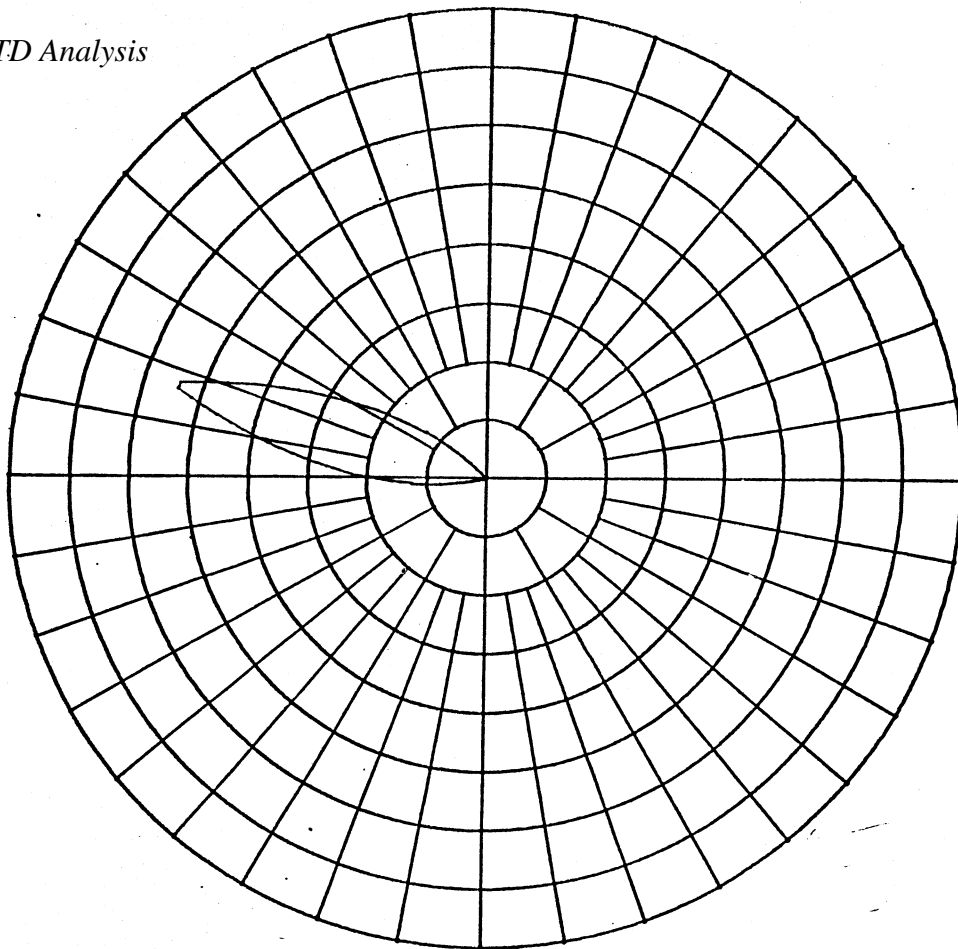
$$E_z^d = \frac{e^{-jks}}{2\sqrt{s}} \left[\frac{1}{jk} \frac{\partial D_s}{\partial \phi'} \right] \left[\frac{e^{-jkR_0} \pi}{R_0^{3/2} \sin(2\alpha)} \right]$$

Because there is grazing incidence on the edge, the direct and reflected rays are the same and the diffractions must be divided in half because the direct + reflected ray has been reduced by a factor of $\frac{1}{2}$. The amplitudes of the slope diffractions in the far field are plotted on page 747.

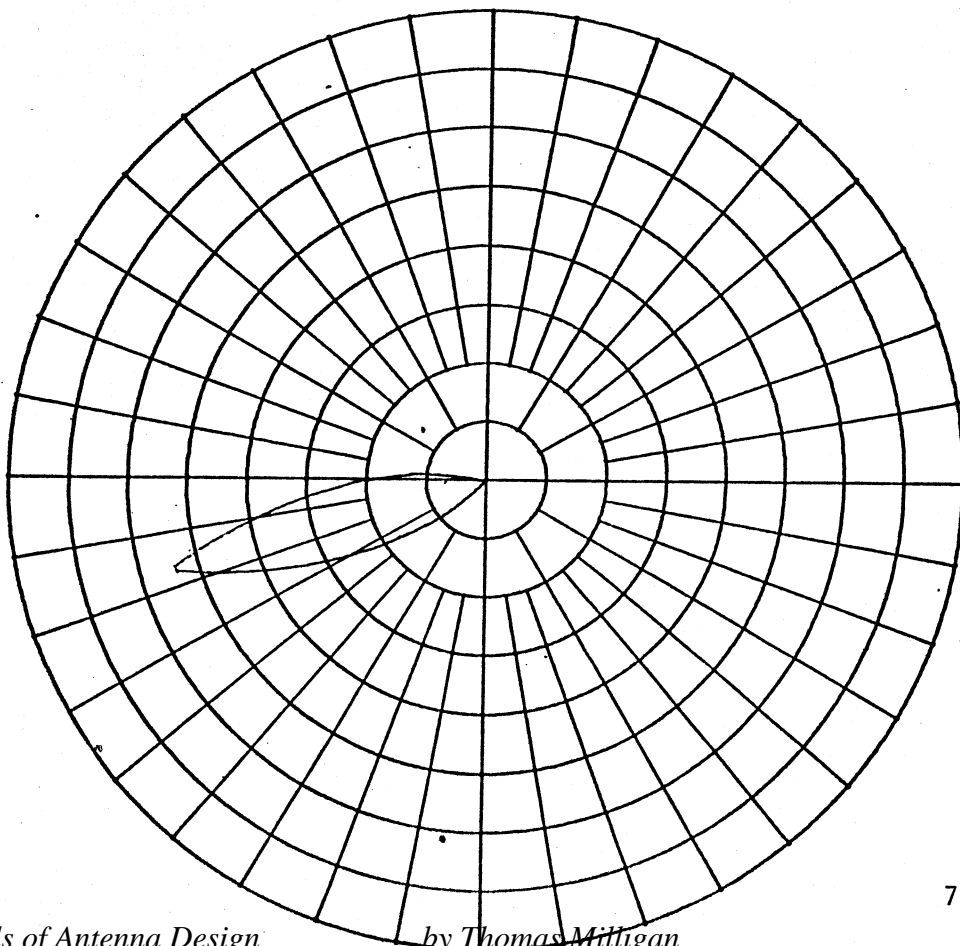
We will only consider the far field. The distance parameter, L , becomes R_0 and we can separate out the term

$$\frac{e^{-jkR}}{\sqrt{R}}$$

Edge Slope Diffraction



Edge Slope Diffraction



We analyze the horn as a three element array with the phase reference at the vertex as was discussed on page 734. The total field including the array factors is given by

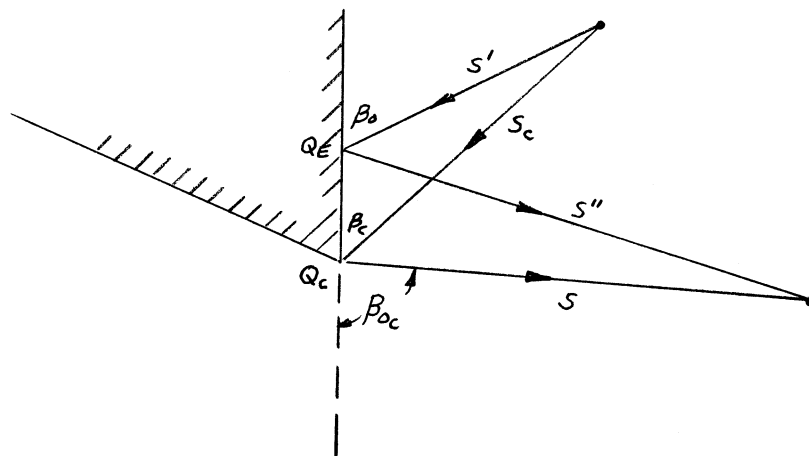
$$E_z = E_{z0} \left(1 + \frac{e^{-jkR_0}}{j^2 k R_0^{3/2}} \frac{\pi}{\sin(2\alpha)} \left[\frac{\partial D_s}{\partial \phi'}(R_0, \pi - \alpha + \theta, 0, z) e^{jkR_0 \cos(\theta - \alpha)} + \frac{\partial D_s}{\partial \phi'}(R_0, \pi - \alpha - \theta, 0, z) e^{jkR_0 \cos(\theta + \alpha)} \right] \right) \frac{e^{-jkR}}{\sqrt{R}}$$

Each term radiates only over a limited region. The diffraction terms are shadowed by the horn. The G.O. field, i.e., is restricted to the flare angle. The combination is plotted on page 749. For comparison, the pattern obtained by aperture integration is drawn on page 750. The GTD solution is quite close. The small sidelobes at $\pm 90^\circ$ on the aperture integration solution are beyond the region of validity. The GTD solution as given does not predict the backlobe because we ignored the E plane edge diffractions.

CORNER DIFFRACTION

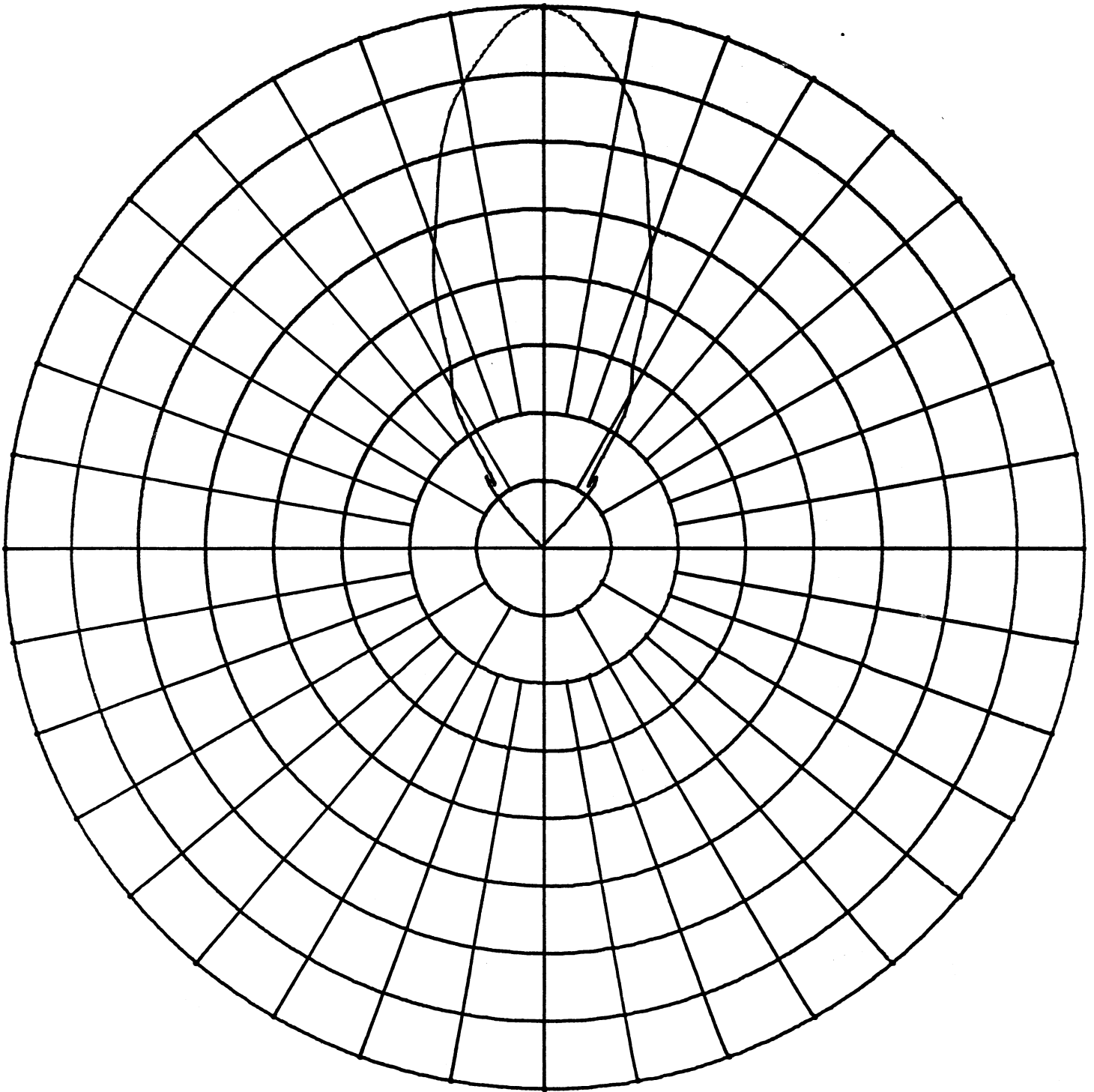
Any time there is a discontinuity in a structure, it becomes a new source of diffracted fields. All the examples given so far have been reduced to two dimensions where there are no ending of the edges. When we consider three dimensional structures, there are corners. These are new sources of diffractions. The diffractions are associated with edges which have been terminated. Edge diffraction is handled as always but there is an additional term due to the corner. Since each corner arises from two edges, there will be a corner diffraction associated with each one. Corner diffraction is in all directions and is not bounded to a cone like the edge diffraction.

Consider the corner diffraction associated with an edge.



Corner diffraction is worked out for an incident spherical wave on a straight edge and has been formulated in terms of equivalent currents.

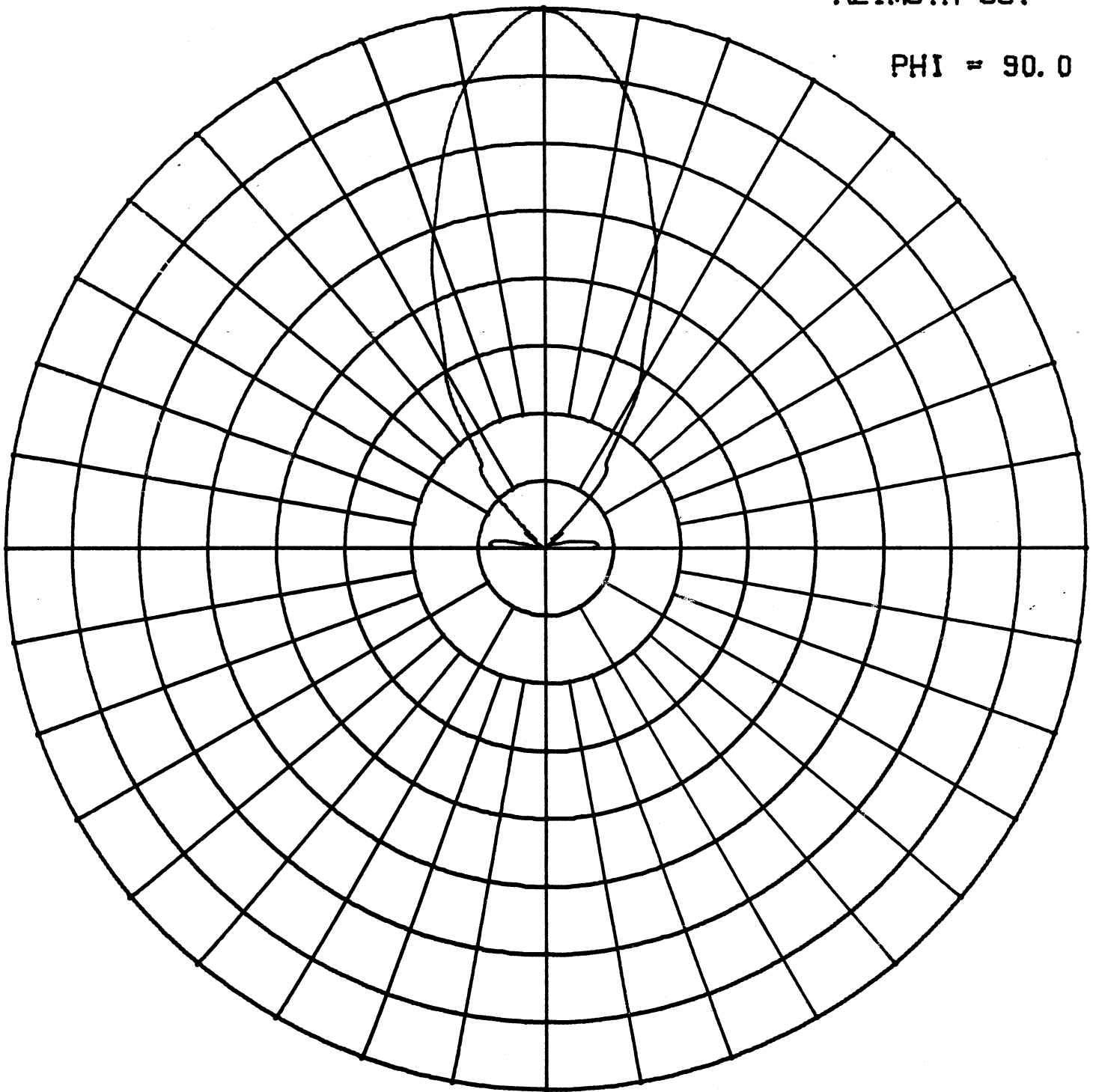
Total H Plane Pattern of Horn



H Plane Pattern of Horn; using Aperture Integration

AZIMUTH CUT

$\text{PHI} = 90.0$



$$\begin{bmatrix} E_{\beta_0}^c \\ E_{\phi_0}^c \end{bmatrix} = \begin{bmatrix} I & Z_0 \\ M & Y_0 \end{bmatrix} \frac{\sqrt{\sin \beta_c \sin \beta_{0c}}}{(\cos \beta_{0c} - \cos \beta_c)} F(K L_c a(\pi + \beta_{0c} - \beta_c)) \frac{e^{-jks}}{4\pi s}$$

$$\begin{bmatrix} I \\ M \end{bmatrix} = - \begin{bmatrix} E_{\beta_0}^i(Q_c) \\ E_{\phi_0}^i(Q_c) \end{bmatrix} \begin{Bmatrix} C_s(Q_E) Y_0 \\ C_h(Q_E) Z_0 \end{Bmatrix} \sqrt{\frac{8\pi}{K}} e^{-j\pi/4}$$

$E_{\beta_0}^i$ and $E_{\phi_0}^i$ are the incident spherical waves on the corner. Z_0 is the impedance of free space and Y_0 is the admittance. The distance parameter L_c is given by

$$L_c = \frac{S_c S}{S_c + S}$$

The soft and hard corner diffraction coefficients are evaluated at Q_e , the point of edge diffraction to the same point.

$$C_{s,h} = \frac{-e^{-j\pi/4}}{2\sqrt{2\pi K} \sin \beta_0} \left[\frac{F(K L a(\phi - \phi'))}{\cos((\phi - \phi')/2)} \left| F\left\{ \frac{L a(\phi - \phi')/\lambda}{K L_c a(\pi + \beta_{0c} - \beta_c)} \right\} \right| \right. \\ \left. + \frac{F(K L a(\phi + \phi'))}{\cos((\phi + \phi')/2)} \left| F\left\{ \frac{L a(\phi + \phi')/\lambda}{K L_c a(\pi + \beta_{0c} - \beta_c)} \right\} \right| \right]$$

The function $a(x) = 2 \cos^2(x/2)$ and the distance parameter $L = \frac{S' S'' \sin^2 \beta_0}{S' + S''}$

The corner diffraction occurs only when the edge is visible to both the source and receiver. If both edges are visible, then there is a contribution from each. The absolute value of the transition functions assures that there is not a sudden jump when it passes through a shadow boundary.

It is necessary in any three dimensional problem to include corner diffraction. As the source and receiver become further and further away, the corner diffractions start to dominate over edge diffractions since it is derived from equivalent currents which are valid at the caustic.

EQUIVALENT CURRENTS

GTD fails to predict fields at caustics. Usually the loss of the possibility of calculating a few points is unimportant. But in those cases where it is required, equivalent currents can be used. It is important to realize that the equivalent current concept can be used everywhere and not just at caustics. It is easier to use edge diffraction coefficients for most points. Edge diffractions are replaced by equivalent edge currents as sources. This process requires line integrals along the edges. Edge currents can also be used to predict the diffractions from a finite length edge although corner diffraction coefficients have eliminated their need here. Corner diffraction coefficients were derived from equivalent currents.

Equivalent currents are postulated that would give the same diffracted fields from an infinite edge by using vector potentials as would diffraction coefficients. Because we use an infinite structure to derive the fields, it reduces the three dimensional problem to two dimensions. On page 721 we derived edge diffraction in terms of Z directed electric and magnetic fields which use soft and hard diffraction coefficients, respectively. The solution of the two dimensional fields derived from vector potentials leads to a scalar potential similar to waveguide expansions which is only in the Z direction. Because the fields are radiated radially outward, only the Hankel function of the second kind is used to describe the fields.

$$\psi_A = \frac{I}{4j} H_0^{(2)}(kp) \quad \psi_F = \frac{M}{4j} H^{(2)}(kp)$$

I is the electric current, M is the magnetic current. The large argument approximation is used to equate the fields derived from these potentials to the two dimensional diffracted fields.

$$E_z^d = E_z^i D_s \frac{e^{-jks}}{\sqrt{s}} \quad H_z^d = H_z^i D_h \frac{e^{-jks}}{\sqrt{s}}$$

When the Z directed electric and magnetic fields derived from the potentials are equated to the diffracted fields, we can solve for the equivalent currents.

$$I = \frac{-2j}{\eta k} E_z^i D_s \sqrt{2\pi k} e^{j(\pi/4)}$$

$$M = \frac{-2j\eta}{k} H_z^i D_h \sqrt{2\pi k} e^{j(\pi/4)}$$

The equivalent currents can be related to the ray fixed incident fields by using the parallel and perpendicular components in the incidence plane.

$$I = \frac{2j}{\eta k} E_{\beta'}^i D_s \sqrt{2\pi k} e^{j(\pi/4)}$$

$$M = \frac{2j}{k} E_{\phi'}^i D_h \sqrt{2\pi k} e^{j(\pi/4)}$$

The vector potentials are found by integrating the currents along the edges.

$$\bar{A} = \int \frac{\bar{I}' e^{jk|\bar{r}-\bar{r}'|}}{4\pi|\bar{r}-\bar{r}'|} \cdot d\bar{q}' \quad \bar{F} = \int \frac{\bar{M}' e^{jk|\bar{r}-\bar{r}'|}}{4\pi|\bar{r}-\bar{r}'|} \cdot d\bar{\ell}'$$

The fields calculated from these potentials are no longer geometrical optics fields and therefore are free of caustics.

$$\bar{E} = -j\omega\mu\bar{A} + \frac{1}{j\omega\epsilon}\nabla(\nabla\cdot\bar{A}) - \nabla\times\bar{F}$$

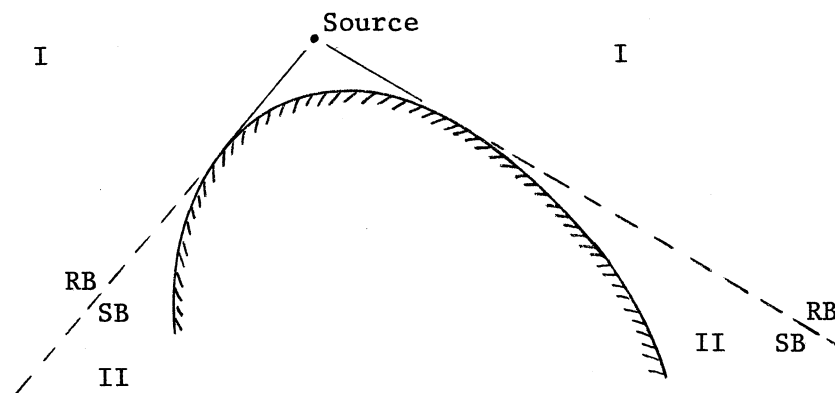
$$\bar{H} = \nabla\times\bar{A} - j\omega\epsilon\bar{F} + \frac{\nabla(\nabla\cdot\bar{F})}{j\omega\mu}$$

In comparison to the rest of GTD these seem cumbersome, but they eliminate caustic problems such as the backlobe of a parabolic reflector when the whole rim lights up and not just two points. Another important point is that the equivalent currents can also be found for slope diffraction coefficients. Remember that these are not real currents because their size depends on the direction of the field point.

DIFFRACTION FROM CURVED SURFACES

One method of considering diffractions is to think of surface waves. Surface wave antennas can be analyzed as radiating only from discontinuities. Between them the wave is bound to the surface (see page 357). The difficult part was finding the radiation pattern from each discontinuity. Diffraction coefficients are the radiation patterns. The edge of a wedge or the end of an edge at a corner are types of discontinuities we have already considered. We can also consider a curved surface as a discontinuity which will radiate energy from a bound surface wave. Normally a perfect conductor cannot support a surface wave, but when considering GTD, it is a handy concept. A wave is bound to a surface by slowing the wave (see page 363), but the wave traveling on the surface of a conductor is not bound because the phase velocity of the wave remains the same as free space.

If there is a source near a curved surface, then space is divided into two regions as shown below. As discussed on page 705, the shadow and reflection

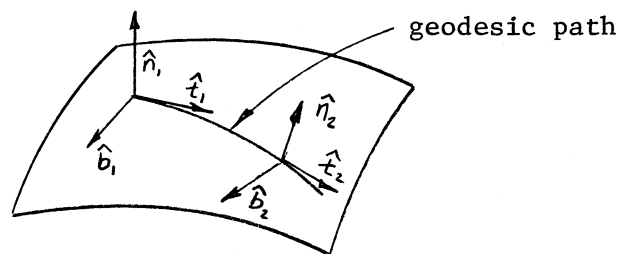


are the same. The transition between the two regions must be continuous. To achieve this we will combine the reflected and diffracted fields in region I so that there will be continuity with an only diffracted field in region II at the boundary. Wedge diffractions were expressed by a single expression which was valid in all regions. The functions are discontinuous but a single expression is used. For diffractions from curved surfaces, different expressions are used in the two regions but with a requirement of continuity across the shadow/reflection boundary.

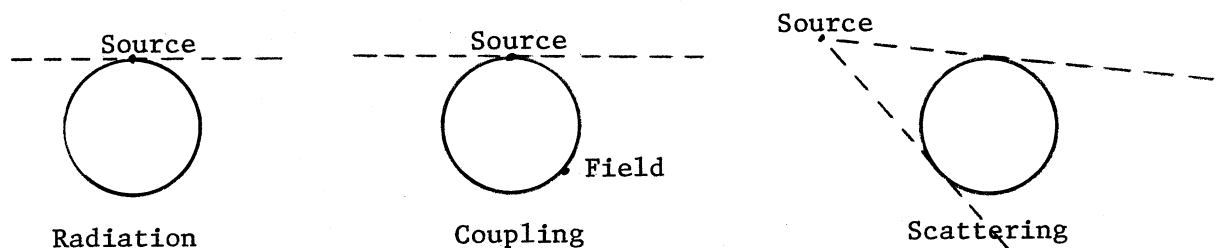
The wave which propagates along the surface sheds energy tangentially. It travels from the source to the shed point along a geodesic. A geodesic is a curve of minimum distance between two points on a surface. In differential geometry it has a broader meaning but for our purpose, the minimum distance definition will serve. We will express the field in terms of ray fixed coordinates along the surface wave. The first coordinate is the normal to the surface, \hat{n} . A binormal vector, \hat{b} , is defined orthogonal to \hat{n} and to a tangent vector on the surface, \hat{t} , such that they form a vector triad.

$$\hat{n} \times \hat{b} = \hat{t}$$

\hat{t} is in the direction of the ray. On a general surface the direction of all three vectors changes as the wave moves along the geodesic. A surface path which has a changing binormal vector is said to have torsion.



Radiation in the presence of a curved surface is divided into three types of problems: radiation, coupling, and scattering. The type of problem depends on the location of the source and field measurement point. A radiation problem has the source located on the curved surface and the field point is located off the surface. This could be an antenna mounted on a missile or aircraft. The second problem is coupling. Both the source antenna and the receiving antenna are mounted on the surface. We can use this to find the mutual coupling between two antennas on a vehicle. The scattering case has the source antenna located off the surface and the field point is on or off the surface. We can approximate the other two problems with the scattering formulation by locating the source antenna slightly off the surface. These three problems are diagrammed below on circular cylinders.



In radiation and coupling problems the source point locates a tangent plane which separates the lit and shadow regions. The radiation from the source is either from an aperture or a short monopole. The aperture is replaced with a magnetic current as was done on page 176 by using the equivalence theorem. The aperture is replaced with an electric conductor (see bottom

of page 177). In this case we do not use the method of images and the magnetic current associated with a differential area is given by

$$\bar{M}(Q') da' = \bar{E}_a(Q') \times \bar{n}' da'$$

Q' is a point in the aperture, \bar{E}_a is the electric field, and \bar{n}' is the unit normal vector. The magnetic current multiplied by a differential area defines a magnetic current moment.

$$\bar{M}(Q') da' = d\bar{p}_m(Q') = \bar{E}_a(Q') \times \bar{n}' da'$$

Similiarly we can have a short monopole on the surface which is used to define short electric moments.

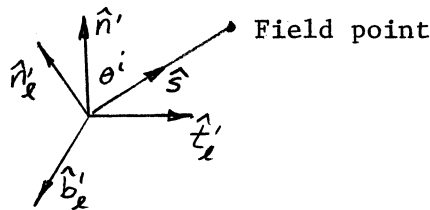
$$d\bar{p}_e(Q') = I(l') dl' \bar{n}'$$

The total length of the monopole is assumed to be short with respect to the radii of curvature; otherwise we have a scattering problem. The electric field of the source is found by integrating over these current moments.

In the shadow region the ray leaves the surface tangentially and has electric fields in directions given by \hat{n}_2 and \hat{b}_2 shown in the diagram above with the direction of propagation given by \hat{t}_2 . The directions in the lit region are ray fixed also. The direction to the lit region field point is \hat{s} . Two vectors are defined normal to this. \hat{b}'_x is the binormal in the surface. The vector product will give us a normal to both of these.

$$\hat{n}' = \hat{b}' \times \hat{s}$$

\hat{s} is at an angle θ^i with respect to the surface normal. The three vectors \hat{n}' , \hat{b}'_x , and \hat{t}'_x still form a vector triad with \hat{n}' as the surface normal and \hat{t}'_x as the tangent vector in the surface. \hat{s} and \hat{t}'_x lie in a plane defined by the binormal, \hat{b}'_x .



The differential electric field in a lit region due to a magnetic or electric moment is given by

$$d\bar{E}_m = \frac{jk}{4\pi} d\bar{p}_e(Q') \cdot \bar{T}_m^e \frac{e^{-jks}}{s}$$

$$\begin{aligned} \bar{T}_m^e = & \hat{b}'_x \hat{n}_x (H^e(\xi^e) + T_o^2 F \cos \theta^i) + \hat{t}'_x \hat{n}_x T_o F \cos \theta^i + \hat{b}'_x \hat{b} T_o F \\ & + \hat{t}'_x \hat{b} (S^e(\xi^e) - T_o^2 F \cos^2 \theta^i) \end{aligned}$$

$$\bar{T}_e^l = z \sin \theta^i [\hat{n}' \hat{n}_r (H^l(\xi^l) + T_0^2 F \cos \theta^i) + \hat{n} \cdot \hat{b} T_0 F]$$

The creeping wave in the shadow region sheds tangentially from the surface. The differential electric field at the field point is given by

$$d\bar{E}_e^m = \frac{jk}{4\pi} d\bar{P}_e^m \cdot \bar{T}_m^l \sqrt{\frac{d\psi_0}{d\eta(Q)}} \left[\frac{\rho_g(Q)}{\rho_g(Q')} \right]^{1/6} e^{-jkt} \sqrt{\frac{\rho_2^d}{s^d(\rho_2^d + s^d)}} e^{-jks^d}$$

$$\bar{T}_m^l = \hat{b}' \hat{n} H(\xi) + \hat{b}' \hat{b} T_0 S(\xi) + \hat{t}' \hat{b} S(\xi)$$

$$\bar{T}_e^l = z (\hat{n}' \hat{n} H(\xi) + \hat{n}' \hat{b} T_0 S(\xi)) \quad z = \frac{-jKz_0}{4\pi} \quad z_0 = 377$$

$H^l(\xi^l)$, $H(\xi)$, $S^l(\xi^l)$, and $S(\xi)$ are Fock functions. They are defined by the following integrals in the complex plane.

$$H^l(\xi^l) = \frac{e^{-j(\xi^l)^3/3}}{\sqrt{\pi}} \int_{\infty e^{-j2\pi/3}}^{\infty} \frac{e^{-j\xi^l \tau / w_2'(\tau)}}{e^{-j2\pi/3}} d\tau$$

$$H(\xi) = \frac{1}{\sqrt{\pi}} \int_{\infty e^{-j2\pi/3}}^{\infty} \frac{e^{-j\xi \tau / w_2'(\tau)}}{e^{-j2\pi/3}} d\tau$$

$$S^l(\xi^l) = \frac{-j}{m(Q')} \frac{e^{-j(\xi^l)^3/3}}{\sqrt{\pi}} \int_{\infty e^{-j2\pi/3}}^{\infty} \frac{e^{-j\xi^l \tau / w_2(\tau)}}{e^{-j2\pi/3}} d\tau$$

$$S(\xi) = \frac{-j}{m(Q')} \frac{1}{\sqrt{\pi}} \int_{\infty e^{-j2\pi/3}}^{\infty} \frac{e^{-j\xi \tau / w_2(\tau)}}{e^{-j2\pi/3}} d\tau$$

$$\xi^l = -m_2(Q') \cos \theta^i \quad \xi = \int_{Q'}^Q \frac{m(t')}{\rho_g(t')} dt'$$

w_2 is a Fock type Airy function given by the following integral.

$$w_2 = \frac{1}{\sqrt{\pi}} \int_{\infty e^{-j2\pi/3}}^{\infty - j\epsilon} e^{\tau t - t^3/3} dt$$

$$w_2'(\tau) = \frac{\partial w_2(\tau)}{\partial \tau}$$

$\rho_g(t')$ is the radius of curvature of the surface along the ray path on the geodesic.

$$m(Q) = \left[\frac{k \rho_g(Q)}{2} \right]^{1/3} \quad m_k(Q') = m(Q') \left[1 + T_0^2 \cos^2 \theta^i \right]^{-1/3}$$

The Fock functions are tabulated functions like sine, cosine, or Bessel functions.

$$F = \frac{S^k(\xi^k) - H^k(\xi^k) \cos \theta^i}{1 + T_0^2 \cos \theta^i}$$

T_0 is the torsion factor.

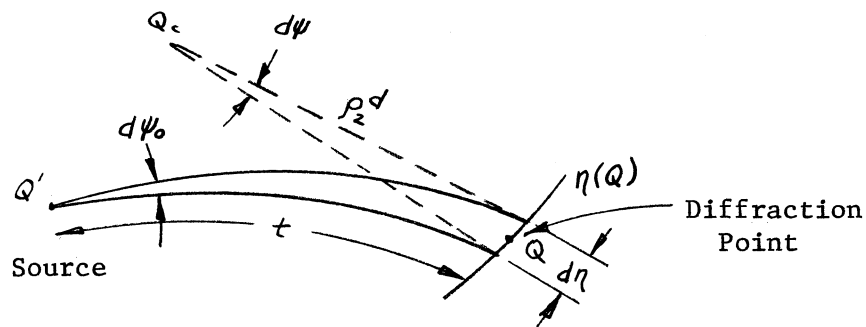
$$T_0 = T(Q') \rho_g(Q')$$

$$T(Q') = \frac{\sin 2\alpha'}{2} \left(\frac{1}{R_2(Q')} - \frac{1}{R_1(Q')} \right) \quad \frac{1}{\rho_g(Q')} = \frac{\cos^2 \alpha'}{R_1(Q')} + \frac{\sin^2 \alpha'}{R_2(Q')}$$

R_1 & R_2 are the principle radii of curvature of the surface with α' the angle between the direction of R_1 and the direction \hat{t} on the surface.

ρ_2^d is the radius of curvature at the diffraction point (tangential shedding) in the direction of the binormal.

One of the caustics of the diffracted field is a line on the surface in the direction of the binormal and is defined by a curve $\eta(Q)$. The rays travel in bundles (ray tube) from the source point. For a differential distance along the curve $\eta(Q)$, the rays come from a differential angle, $d\psi_0$, at the source.



If the torsion is zero or the problem can be described in two dimensions, then these expressions are simplified considerably. To find the total diffracted field it necessary to integrated over the aperture or monopole current moments.

SCATTERING FROM A CURVED SURFACE

Scattering is divided into lit and shadow regions with the requirement of continuity across the shadow boundary. In the lit region we have a direct ray plus a reflected ray.

$$\bar{E}^i(P_L) + \bar{E}^i(Q_R) \cdot \bar{\bar{R}} \sqrt{\frac{\rho_1^r \rho_2^r}{(\rho_1^r + s^r)(\rho_2^r + s)}} e^{-jk s^r}$$

ρ_1^r and ρ_2^r are the principle radii of curvature of the reflected ray given on page 716. Q_R is the point of reflection and s^r is the distance to the field point.

The reflection dyadic, $\bar{\bar{R}}$, is modified to provide a smooth transition at the shadow boundary. It reduces to the standard reflection dyadic far from the boundary.

$$\bar{\bar{R}} = R_s \bar{a}_\perp \bar{a}_\perp + R_h \bar{a}_\parallel \bar{a}_\parallel$$

$$R_{s,h} = - \left[\sqrt{\frac{-4}{\xi^L}} e^{-j(\xi^L)^3/12} \left(\frac{e^{-j\pi/4}}{2\sqrt{\eta \xi^L}} [1 - F(\chi^L)] + \hat{P}_s^h(\xi^L) \right) \right]$$

F is the transition function used with edge diffraction.

$$X^L = 2 k L^L \cos^2 \theta^i$$

$$L^L = \frac{(\rho_1^i + s_o)(\rho_2^i + s_o)}{(\rho_1^i + s_o + s)(\rho_2^i + s_o + s)} - \frac{s(\rho_2^r + s)}{\rho_2^r}$$

For cylindrical or spherical wave incidence this is reduced.

$$L^L = \frac{s^i s^r}{s^i + s^r}$$

$P_{s,h}(\xi^L)$ are called the Pekeris caret functions.

$$\hat{P}_s(\chi) = \frac{1}{\sqrt{\pi}} \int_{-\infty}^{\infty} \frac{V(\tau)}{W_2(\tau)} e^{-j\chi\tau} d\tau$$

$$\hat{P}_h(\chi) = \frac{1}{\sqrt{\pi}} \int_{-\infty}^{\infty} \frac{V'(\tau)}{W_2'(\tau)} e^{-j\chi\tau} d\tau$$

$$2j V(\tau) = W_1(\tau) - W_2(\tau) \quad V'(\tau) = \frac{\partial V(\tau)}{\partial \tau}$$

ξ^L is defined on page 756.

The diffracted field in the shadow region is given by

$$\bar{E}^d = \bar{E}^i(Q_i) \cdot \bar{\bar{T}} \sqrt{\frac{\rho_2^d}{s^d(\rho_2^d + s)}} e^{-jk s^d}$$

One caustic of the diffracted field is on the surface at the diffraction point (tangential shedding), ρ_2^d is the caustic distance in the other plane.

$$\vec{T} = T_s \hat{b}_1 \hat{b}_2 + T_h \hat{n}_1 \hat{n}_2$$

Point 1 is the attachment point of the incoming wave and 2 is the diffraction point.

$$T_{s,h} = - \left[\sqrt{m(Q_1)m(Q_2)} \sqrt{\frac{2}{k}} \left\{ \frac{e^{-j\pi/4}}{2\sqrt{\pi\xi}} [1 - F(x^d)] + \hat{P}_{s,h}(\xi) \right\} \sqrt{\frac{d\eta(Q_1)}{d\eta(Q_2)}} e^{-jk t} \right]$$

t is the length along the surface from attachment point Q_1 to diffraction (or shedding) point Q_2 . η is the curve along the binormal and

$$\sqrt{\frac{d\eta(Q_1)}{d\eta(Q_2)}}$$

is a measure of the spreading along the surface wave. m is defined on page 757 in terms of the surface radius of curvature. F is the transition function and $\hat{P}(\xi)$ is the Pekeris function.

$$x^d = \frac{k L^d \xi^2}{2 m(Q_1) m(Q_2)}$$

$$L^d = \frac{(\rho_1^i + s_o)(\rho_2^i + s_o)}{(\rho_1^i + s_o + s)(\rho_2^i + s_o + s)} \frac{s(\rho_2^r + s)}{\rho_2^r}$$

For spherical or cylindrical wave input:
 ξ is given on page 756.

$$L^d = \frac{s_o s^d}{s_o + s^d}$$

These equations are rather involved but easily handled in a computer routine. The geometry of any configuration is the largest part of the problem. Given a general curved surface there is no formula to find the location of the attachment point and shedding point at the end of a geodesic curve which will join a given source point to a given field point. Usually a known diffraction is picked and other points are found by incrementing along the curve by small steps until the points are found.

P. H. Pathak, W. D. Burnside, and R. J. Marhefka, "A Uniform GTD Analysis of the Diffraction of Electromagnetic Waves by a Smooth Convex Surface", IEEE Trans. on Antennas & Propagation, Sept. 1980.

P. H. Pathak, N. Wang, W. D. Burnside, and R. G. Kouyoumjian, "A Uniform GTD Solution for the Radiation from Sources on a Convex Surface", IEEE Trans. on Antennas & Propagation, July 1981.